(Takizawa *et al.* 2001). Regulation of the DNA methylation is thus very important for astrocyte differentiation, which is programmed to start at a relatively late stage of brain development. However, there is not enough information about the role of DNA methylation in the regulation of lineage specification of neural stem cells during the early period of neural development when the neuroectoderm is formed. In order to solve this problem, we established an *in vitro* neural differentiation-inducing culture system using mouse embryonic stem (ES) cells (Shimozaki *et al.* 2003). Neural differentiation from the ES cells was found to occur in a manner similar to that observed in neurogenesis *in vivo* (Kawasaki *et al.* 2000; Shimozaki *et al.* 2003). Here, we report that the CpG dinucleotide in the STAT3 binding site in the GFAP promoter exhibits a high incidence of cytidine-methylation in undifferentiated ES cells. We also show that the high incidence of methylation of this cytidine is maintained in ES cell-derived neuroectoderm-like cells, but it undergoes demethylation when the cells become competent to differentiate into GFAP-positive astrocytes. This is the first report to analyze DNA methylation and demethylation of a specific site in a gene promoter expressed in somatic tissues derived from ES cells.

Materials and methods

Cell culture and animals

Undifferentiated ES cells (D3, CP1, CGR8, CCE and OEf1P) were maintained in an undifferentiated state on gelatin-coated dishes as described previously (Shimozaki *et al.* 2003). For *in vitro* differentiation, we used the OEf1P ES cells, which are derived from E14tg2a cells, and contain an IRES-puromycin-pA cassette in the downstream of the Oct3/4 gene (Niwa *et al.*, unpublished). For sphere formation, ES cells were cultured on poly-hydroxy-ethyl methylacrylate (poly-HEMA)-coated dishes in Glasgow minimum essential medium (G-MEM) medium supplemented with 10% knockout serum replacement Gibco-BRL, Rockville MD, USA) [for neural spheroids (NSs)] or 10% fetal bovine serum [for embryoid bodies (EBs)], 2 mM glutamine, 1 mM pyruvate, 0.1 mM nonessential amino acids and 0.1 mM 2-mercaptoethanol. Medium changes were performed on day 4 and then every 2 days thereafter. After the sphere culture, the aggregates were washed with phosphate-buffered saline, and then treated with trypsin-EDTA (Gibco-BRL) to dissociate the cell aggregates. The dissociation was stopped by treatment with a trypsin inhibitor and the cells were plated onto poly L-ornithine/fibronectin-coated dishes. The cells were cultured for 4 days in N2-supplemented Dulbecco's modified Eagle's medium/F-12 medium containing 10 ng/mL of basic fibroblast growth factor (R & D Systems, Minneapolis, MN, USA) in the presence or absence of 10% fetal bovine serum with or without 80 ng/mL of leukemia inhibitory factor (LIF, Gibco-BRL). The cells in the first 4-day monolayer culture starting from NS4 were cultured in the N2-medium described above containing 10% knockout serum replacement with or without LIF. Time-pregnant ICR mice were used to prepare neuroepithelial cells, fibroblasts and hepatocytes. Mice were treated according to the guidelines of the Kumamoto University Center for Animal Resources and Development. Neuroepithelial cells were prepared from the telencephalons of E14.5 mice and cultured as described previously (Nakashima *et al.* 1999b). Fibroblasts were prepared from the ventral skin of E14.5 mice. For preparation of hepatocytes, the livers of E14.5 mice were minced and cultured for 16 h on collagen I-coated dishes in GMEM supplemented with 10% fetal bovine serum, 2 mM glutamine, 1 mM pyruvate, 0.1 mM nonessential amino acids and 0.1 mM 2-mercaptoethanol. After washing with phosphate-buffered saline, the cells attached to the dishes were cultured.

Immunocytochemistry

Immunofluorescent staining was performed with the following antibodies: an anti-microtubule-associated protein 2 (MAP2) monoclonal antibody (Sigma, St Louis, MO, USA) and an anti-GFAP polyclonal antibody (Dako, Carpinteria, CA, USA). The following secondary antibodies were used: an Alexa 488-conjugated goat anti-mouse IgG antibody (Molecular Probes, Eugene, OR, USA), and a rhodamine-conjugated donkey anti-rabbit IgG antibody (Chemicon, Temecula, CA, USA). The cells were counterstained with Hoechst 33258 to identify the nuclei. Images were obtained using an AX70 fluorescence microscope (Olympus, Tokyo).

RNA analysis

For RT–PCR analysis, we performed oligo-dT-primed reverse transcription on aliquots (5 μg) of total RNA and used 1/100 of the resultant single-stranded cDNA products for each PCR amplification. The primer sets with which all cDNAs were amplified in a quantifiable range are listed in Table 1.

Bisulfite sequencing

The genomic DNA from each culture was prepared as described (Clark *et al.* 1994). For bisulfite sequencing, 5 μg of genomic DNA was digested with *Sac*I. After denaturing with 0.3 M NaOH, the samples were treated with 3.1 M sodium bisulfite and 0.5 mM hydroquinone at 55°C for 16 h. The samples were incubated with 3 M NaOH and neutralized by the addition of 3 M ammonium acetate. After purification, the DNA samples containing the STAT3 recognition sequence were amplified by PCR and sequenced as described previously (Takizawa *et al.* 2001). The average methylation frequency in every cell type was calculated based on the frequency values derived from the two independent bisulfite sequencing experiments. Eleven to 14 sequencing analyses were performed for each bisulfite-treated sample.

Immunoblotting

Cells were lysed by sonication in NP-40 lysis buffer: 0.5% NP-40, 10 mM Tris-HCl pH 7.4, 150 mM NaCl, 1 mM pAPMSF (Wako Pure Chemicals, Osaka, Japan), 10 μg/mL aprotinin (Sigma), 2 mM sodium orthovanadate (Wako Pure Chemicals) and 5 mM EDTA. The lysates were immunoprecipitated with anti-STAT3 antibodies (Transduction Laboratories, Lexington, KY, USA). Immunoprecipitates and lysates were subjected to sodium dodecyl sulfate–polyacrylamide gel electrophoresis and subsequent immunoblotting with antibodies against STAT3 (Transduction Laboratories) and tyrosine-phosphorylated STAT3 (Cell Signaling, Beverly, MA, USA). Detection was performed using the ECL detection system (Amersham, Piscataway, NJ, USA).

Table 1 Gene-specific PCR primers

Gene	Forward primer	Reverse primer	Size of product (bp)
Fgf5	AAAGTCAATGGCTCCCACGAA	AGAGGCTGTAGAACATGATT	464
AFP	CAAAGCATTGCACGAAAATG	TAAACACCCATCGCCAGAGT	471
Emx2	TTCGAACCGCCTTCTCGCCG	TGAGCCTTCTTCCTCTAG	188
Otx1	GCAGCGACGGGAGCGCACCA	TGCTGCTGGCGGCACTTGGC	180
Mash1	CGTCCTCTCCGGAACTGAT	TCCTGCTTCCAAAGTCCATT	483
CK-17	CCTGCTCCAGATTGACAATG	CTTGCTGAAGAACCAGTCTTC	380
Brachyury	ATGCCAAAGAAAGAAACGAC	AGAGGCTGTAGAACATGATT	834
GAPDH	ACCACAGTCCATGCCATCAC	TCCACCACCCTGTTGCTGTA	452

Results

The critical STAT3 binding site in the glial fibrillary acidic protein gene promoter is methylated in embryonic stem cells

In the mouse, rat and human GFAP gene promoters, a STAT3 recognition element (TTCCGAGAA, −1518 to −1510 in the mouse promoter; Fig. 1) is well conserved, and this element is critical for expression of the GFAP gene (Bonni *et al.* 1997; Nakashima *et al.* 1999b). We investigated the methylation status of this STAT3 binding site in the GFAP gene promoter in five ES cell lines using a bisulfite sequencing method (Clark *et al.* 1994). Each ES cell line exhibited a high frequency of methylation of the cytosine residue in the CpG dinucleotide in the STAT3 recognition element in the GFAP gene promoter (Fig. 1). Methylation of this CpG site has been demonstrated to inhibit the expression of GFAP. It is reasonable to note that these ES cells did not express the GFAP gene (data not shown), even though the cells were maintained with a STAT3-activating cytokine, LIF.

Establishment of an *in vitro* neural inducing system from embryonic stem cells

We wanted to analyze the DNA methylation status in ES cells that were in the process of development. For this purpose, ES cells that had been maintained in the presence of LIF and fetal bovine serum were dissociated from culture dishes, and washed several times to remove residual LIF and fetal bovine serum. The ES cells were then cultured in serum-free LIF-deficient medium (neural spheroid, NS culture) or serum-containing LIF-deficient medium (embryoid body, EB culture) on poly-HEMA-coated dishes to make floating cultures. After 4 days, the shapes of the spheres formed in the serum-free LIF-deficient medium (NS4; Fig. S1a) and the serum-containing LIF-deficient culture (EB4; Fig. S1c) were very similar. However, after 8 days (data not shown) and 14 days (Figs S1b and d), the shapes of the spheres in the NS and EB cultures were different. In contrast to the neurosphere-like structures in the serum-free LIF-deficient medium (NS14; Fig. S1b), the cell aggregates in the serum-containing LIF-deficient culture (EB14; Fig. S1d) exhibited embryoid body-like spheres. We examined the expressions of several differentiation marker genes in each culture by RT–PCR analysis. In the serum-free LIF-deficient culture, NS14 spheres expressed the neural marker genes *Emx2* (Simeone *et al.* 1992), *Otx1* (Acampora *et al.* 1998) and *Mash1* (Ma *et al.* 1997), but not markers for other cell lineages, namely *AFP* (Dziadek and Adamson 1978) (visceral endoderm), *CK-17* (McGowan and Coulombe 1998) (epidermis), and *Brachyury* (Wilkinson *et al.* 1990) (mesoderm) (Fig. 2). In contrast, in the serum-containing LIF-deficient culture, EB14 spheres expressed all the differentiation marker genes tested, as the formation of embryoid bodies after withdrawal of LIF/gp130 signaling leads to the formation of a variety of differentiated cell populations, which can include all the embryonic and adult cell populations (Bradley *et al.* 1984; Doetschman *et al.* 1985).

To obtain GFAP-positive astrocytes from ES cells, the spheres were subjected to monolayer cultures and stimulated with LIF, as LIF/gp130 signaling effectively induces GFAP-expressing astrocytes from neural progenitors. In this experiment, the spheres formed in the floating cell cultures were dissociated with trypsin, and then plated onto poly L-ornithine/fibronectin-coated dishes in serum-free N2 medium (N2-supplemented Dulbecco's modified Eagle's medium/F-12 with basic fibroblast growth factor and LIF) (for NS cultures) or serum-containing N2 medium without LIF (for EB cultures) for 4 days. We did not detect any GFAP-positive astrocytes after a 4-day monolayer culture

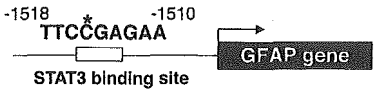

Methylation Frequency in the STAT3 Binding Site in the GFAP Promoter

ES cells	D3	CP1	CGR8	CCE	OEf1P
Methylated CpG	19	22	20	20	21
n	23	22	22	24	24
Percent	82.6 %	100 %	90.9 %	83.3 %	87.5 %

Fig. 1 Methylation frequency of the STAT3 binding site in the glial fibrillary acidic protein (GFAP) promoter of several embryonic stem (ES) cell lines. The asterisk indicates the CpG methylation site in the STAT3 binding site (−1518 to −1510) in the GFAP promoter. The primary data from the experiments are summarized in the table.

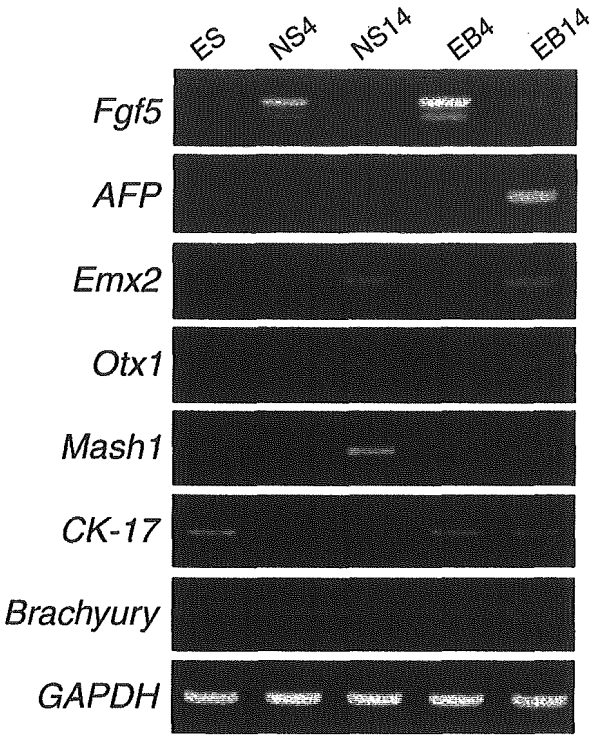

Fig. 2 Differentiation profiling of embryonic stem (ES) cells in suspension culture at days 4 and 14. Total RNA was extracted from each culture, and subjected to RT–PCR analysis of the genes indicated on the left.

starting from NS4 (Fig. 3a). The 4-day monolayer culture starting from NS4 was subjected to dissociation with trypsin followed by another 4-day monolayer culture (Fig. 3e). The cells were then stained for neuronal (MAP2) or astrocytic (GFAP) markers. Most of the cells were positive for MAP2, whereas none were positive for GFAP. A few GFAP-positive astrocytes were observed after the first 4-day monolayer culture starting from the 14 day-sphere culture (NS14) (Fig. 3b). Interestingly, when the cells that had been cultured under this condition were dissociated and subjected to another 4-day monolayer culture, many astrocytes expressing GFAP were detected, whereas only a few MAP2-positive neurons were observed (Fig. 3f). When the cells dissociated from the spheres formed in the serum-containing medium were used for subsequent monolayer cultures, quite different results were obtained. There were no cells expressing MAP2 or GFAP after either the first or the second 4-day monolayer cultures prepared from EB4 (Figs 3c and g). Only a few MAP2- or GFAP-positive cells were observed after monolayer cultures prepared from the EB14 culture that contained serum (Figs 3d and h). These results suggested that the preference of the cell-fate determinator, e.g. for neuronal or astrocytic differentiation, may have been affected by the culture conditions.

We calculated the percentages of MAP2-positive neurons and GFAP-positive astrocytes in the above cultures with or without LIF. After the first 4-day monolayer culture of NS4, only a small number of GFAP-positive astrocytes appeared, even in the presence of the astrocytic differentiation-inducing cytokine LIF (Fig. 3i). In contrast, effective astrogenesis was induced by LIF after the second 4-day monolayer culture of the NS14 culture (48.2%; Fig. 3j). After the second 4-day monolayer culture of the NS4 culture, cells showed continuous neuronal differentiation, but not astrogenesis despite the stimulation by LIF (Fig. 3j). Given that GFAP expression is dependent on STAT3 activation, it was possible that STAT3 was not activated in these monolayer cells upon LIF stimulation. However, as shown in Fig. 3(k), STAT3 protein was expressed and activated in response to LIF stimulation in these *in vitro* differentiated cells. This result suggests that a mechanism other than failure of STAT3 activation underlies the prevention of GFAP expression in these cells.

Demethylation confers responsiveness to gliogenic signaling on neural progenitors from embryonic stem cells

We next examined the CpG methylation status of the STAT3 binding site in the GFAP gene promoter in the cells cultured using the above methods. As shown in Fig. 4(a) (white columns), NS4 exhibited high rates of methylation (95.9%) and the high methylation frequency was maintained during the 4-day monolayer culture (96.3%). These results correlate well with the observation that astrocytes did not appear in these two cell populations. Interestingly, the CpG methylation of this particular STAT3 binding site in NS14 was also very frequent (78.4%; but less than NS4), but became significantly decreased when subjected to the 4-day monolayer culture (41.7%) (black columns; Fig. 4a). As shown in Fig. 3(j), the second monolayer of NS14 cells cultured with LIF produced 48.2% GFAP-positive astrocytes. In contrast, EB4 and EB14 cultures did not show the change in methylation status because EB cultures contained many non-neural cells in which the STAT3 binding site of the GFAP promoter would be hypermethylated. These results suggest the importance of the relationship between astrogenesis and DNA methylation, and that the relationship is well controlled from the pluripotent embryonic stem cell stage.

Finally, to clarify the difference in regulation of the DNA methylation in the STAT3 recognition site in the GFAP promoter between neural and other non-neural cells *in vivo*, we examined the methylation frequency in E14.5 mouse telencephalons, skin and liver. Skin and liver cells, either freshly prepared or cultured for 4 days, showed a high frequency of DNA methylation (Fig. 5). In contrast to these non-neural cells, the methylation frequency of this site in neuroepithelial cells was relatively lower (48.7%), and became even lower (16.7%) after culture for 4 days. In

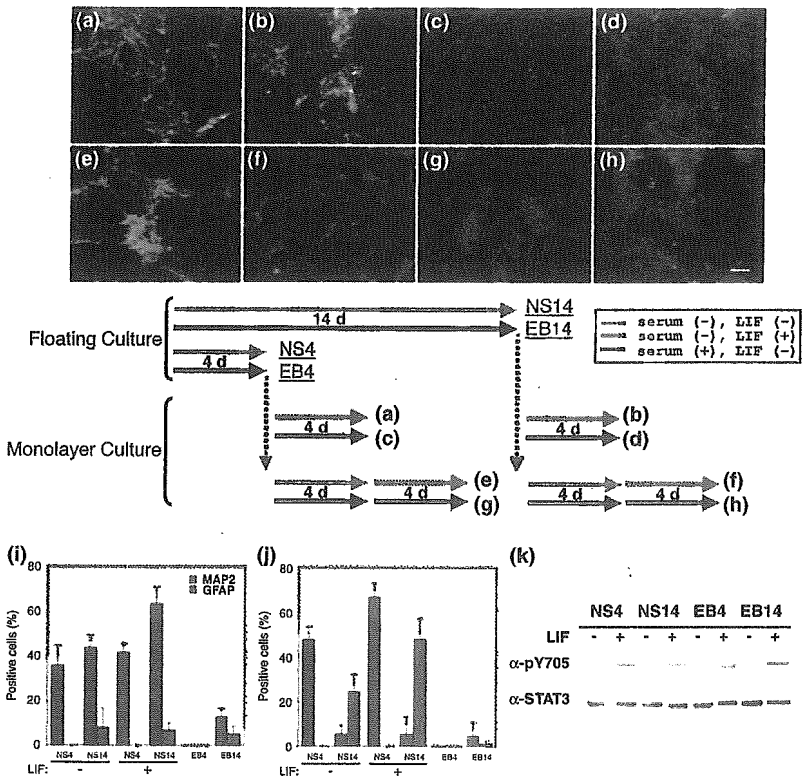

Fig. 3 Culture stage-specific neurogenesis and astrogenesis under the NS neural-inducing sphere culture conditions. NS and EB aggregates were dissociated and seeded onto ornithine/fibronectin (O/F)-coated dishes with leukemia inhibitory factor (LIF) in the absence of serum (for NSs) or without LIF in the presence of serum (for EBs) for 4 days (first 4-day monolayer culture: (a) from 4-day NS spheres; (b) from 14-day NS spheres; (c) from 4-day EB spheres; (d) from 14-day EB spheres. The first 4-day monolayer cultures without LIF starting from spheres were subjected to dissociation with trypsin followed by another 4-day monolayer culture with LIF in the absence of serum (for NSs; e, f) or without LIF in the presence of serum (for EBs; g, h). Cells were stained with anti-MAP2 (microtubule-associated protein 2) antibodies (green), anti-GFAP (glial fibrillary acidic protein) antibodies (red) and Hoechst 33258 (blue). Scale bar, 50 μm. (i, j) NS/EB aggregates or the 4-day monolayers were cultured with or without LIF in the absence of serum (for NSs) or without LIF in the presence of serum (for EBs) for 4 days (i: cells after the first 4-day monolayer culture; j: cells after the second 4-day-monolayer culture). Cells were stained with anti-MAP2 and anti-GFAP antibodies and the frequencies of the positive cells were calculated. Vertical bars indicate the SD. (k) STAT3 activation in each sphere culture. Sphere cells cultured in the presence (EB4, EB14) or absence (NS4, NS14) of serum were dissociated and attached to O/F-coated dishes. Lysates from these cells after incubation with or without LIF (80 ng/mL) for 10 min were subjected to western blotting, and probed with antibodies against tyrosine-phosphorylated STAT3 or STAT3.

E14.5 mouse neuroepithelial cells from embryonic brain, it was reported that the CpG methylation of the STAT3 binding site in the GFAP promoter was dramatically demethylated after 4-day culture (Takizawa *et al.* 2001). The methylation rates in adult tissues (muscle, heart and liver) were calculated previously in the same report, and revealed to be highly methylated. In the present study, we further suggested that there was machinery for cell fate-specific maintenance of methylation as well as demethylation of this particular CpG site. These results suggest that the CpG methylation of the STAT3 binding site in the GFAP gene promoter is well controlled, that is, the CpG dinucleotide is cytidine-methylated in early embryogenesis, and then demethylation occurs during the development of neuroepithelial cells while methylation is maintained for the development of other cell lineages.

Discussion

ES cells can contribute *in vivo* to the formation of all tissues when introduced into blastocysts, and can be induced *in vitro* to acquire the specific phenotypes of the various types of differentiated cell populations. We used OEf1P ES cells that carry the IRES-puromycin resistance gene construct under the Oct3/4 gene, as these cells are easily selected as pluripotent stem cells by puromycin. Furthermore, this ES line showed effective neural differentiation among the lines tested under our culture periods and conditions. In the

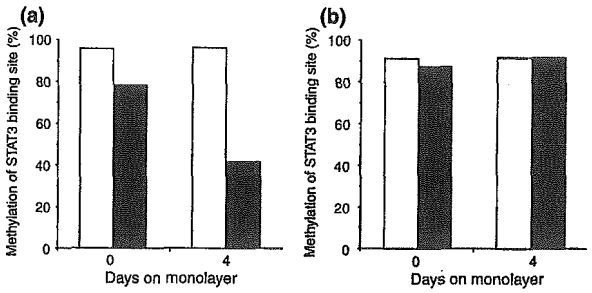

Fig. 4 Culture stage- and condition-specific CpG demethylation of the STAT3 binding site in the glial fibrillary acidic protein (GFAP) promoter. The STAT3 recognition sequence in the GFAP promoter was investigated for its methylation status using a bisulfite sequencing method in NS/EB aggregates or the cells cultured as monolayers for 4 days starting from each aggregate after dissociation with trypsin. The 4-day monolayer starting from the NS aggregates was cultured in serum-free medium, and starting from the EB aggregates it was cultured in serum-containing medium. The average of two independent bisulfite-sequencing experiments with a minimum of 11 clones is shown in the graph. (a) NS4 (white columns) and NS14 (black columns). (b) EB4 (white columns) and EB14 (black columns).

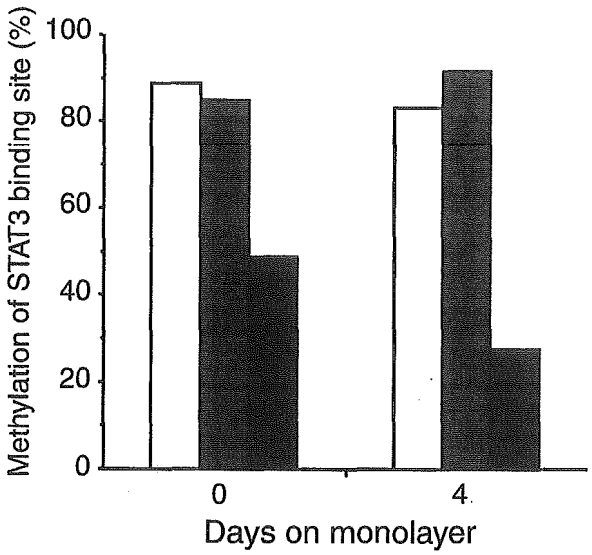

Fig. 5 Neural-specific CpG demethylation of the STAT3 binding site in the glial fibrillary acidic protein (GFAP) promoter. CpG methylation of the STAT3 binding site of the GFAP promoter was analyzed using a bisulfite sequencing method in freshly prepared E14.5 mouse skin (white columns), liver (gray columns) and telencephalon (black columns), or after 4 days of *in vitro* culture. The average of two independent bisulfite-sequencing experiments with a minimum of 11 clones is shown in the graph.

present study, we established an effective neural inducing system from ES cells, in which neural progenitors are easily enriched, presumably because non-neural cells tend to die in the serum-free LIF-deficient floating culture on the poly-HEMA-coated dishes. Our results suggest that the second 4-day monolayer culture is important for neural progenitors to become responsive to astrogenic signals, and we showed that the ability of ES cell-derived neural progenitors to differentiate into astrocytes was dependent on both the sphere and monolayer culture periods (Figs 3a–h). The combination of a relatively long (14-day) floating culture and two successive 4-day monolayer cultures seems to be important for effective astrogenesis in our culture system. The floating culture condition in which cells become aggregated might induce a signal that is involved in the maintenance and/or change in the differentiation competence of neural progenitors. Dissociation of the aggregates and subsequent monolayer culture might contribute to the development of astrocytes.

DNA methylation is one of the best-studied epigenetic modifications of DNA in all unicellular and multicellular organisms. DNA methylation levels in different lineages change temporally during mammalian development. The DNA of the zygote is substantially methylated. During early development, the genome undergoes global demethylation, and in the epiblast lineage it becomes globally re-methylated *de novo* after implantation (Jaenisch 1997). ES cells correspond to a stage of development after the blastocyst stage. The DNA of ES cells is relatively highly methylated, and has high *de novo* methylation activity (Stewart *et al.* 1982). In this report, we showed that the STAT3 binding site in the GFAP gene promoter is highly methylated in ES cells. Demethylation of this site is only programmed when pluripotent cells are committed to a neural lineage that is capable of producing astrocytes. Neural stem cells in the early stage of development have limited ability to differentiate (Qian *et al.* 2000), whereas those in the later stage have much potential, and differentiate into neurons, astrocytes and oligodendrocytes (McKay 1997; Gage 2000). This limitation of differentiation potential in the early stage of development could be due to DNA methylation, as the DNA methylation is thought to repress gene expression. The specific site of DNA demethylation could lead to a chromatin rearrangement suitable for binding transcription factors activated by cell-extrinsic signals with several sequential steps.

LIF/gp130 signaling is very important for the induction of GFAP-positive astrocytes. Therefore, the DNA demethylation of the CpG dinucleotide in the STAT3 binding site in the GFAP gene promoter is required for neural progenitors to proceed with astrogenesis in response to LIF/gp130 signaling. The STAT3 binding site in the GFAP gene is methylated in non-neural cell lineages, and this high frequency of DNA methylation is maintained to the final development of mice (Figs 4b and 5) (Takizawa *et al.* 2001). However, the neural cell fate-specific DNA demethylation and the maintenance of DNA methylation of the STAT3 binding site in the GFAP promoter were not affected by the addition of LIF in either cells differentiated from ES cells or skin, liver and neuro-

epithelial cells from E14.5 mouse embryos (data not shown). To investigate whether GFAP can be induced by LIF in ES cells when this CpG site is demethylated, we tried to culture ES cells with 5-aza-2′-deoxycytidine (5-Aza-CdR), a demethylation reagent. However, due to the high sensitivity of ES cells to the toxic effects of this reagent, the cells readily died and we could not obtain conclusive results (data not shown). It remains unknown whether demethylation in ES cells is directly related to their cell death.

We also investigated the methylation status in the promoter of another astrocyte marker, S100β. Interestingly, the incidence of CpG methylation of a specific site in the S100β promoter was very high in ES cells, but the CpG methylation frequency in this site was low in ES cell-derived neural progenitors that have the ability to undergo astrogenesis (Namihira *et al.* unpublished result). These data suggest that astrocyte gene-specific demethylation is not confined to the GFAP gene promoter, but is also applicable to the S100β gene promoter. The CpG methylation status of the whole genome of ES cells, as analyzed by digestion with a methylated DNA sequence-sensitive restriction enzyme, *Hpa*II, was not dramatically changed in this culture (Fig. S2). Therefore, it is suggested that site-specific demethylation occurs in our neural inducing culture system rather than demethylation in the whole genome. Recently, it was reported that the zinc-finger factor REST/NRSF can mediate both active repression of neuronal-specific genes via recruitment of specific HDACs and gene silencing by recruitment of CoREST complexes to specific promoters in a cell type- and promoter-specific DNA methylation-dependent manner (Lunyak *et al.* 2002). In the control of chromatin during neural differentiation, histone modification and DNA methylation are thought to have a close relationship that would be a key to solving the above problems. Although the mechanism for the regulation of DNA methylation and demethylation caused by cell differentiation is not well understood, the *in vitro* neural inducing system used in this report should contribute to further studies to define the molecules/mechanism concerned with the regulation.

Acknowledgements

We thank Y. Noguchi and M. Ohta for secretarial assistance, and K. Kaneko and Y. Saiki for technical help. We are grateful to H. Niwa for the OEf1P cells. This work was supported by a Grant-in-Aid from the Ministry of Education, Science, Sports and Culture of Japan, the Human Frontier Science Program, and the Virtual Research Institute of Aging of Nippon Boehringer Ingelheim.

Supplementary material

The following material is available from:

http://www.blackwellpublishing.com/products/journals/suppmat/JNC/JNC3031/JNC3031sm.htm

Fig. S1 Morphology of embryonic stem (ES) cells in suspension culture at days 4 and 14.

Fig. S2 CpG methylation status of the whole genome of embryonic stem (ES) cells in differentiation cultures.

References

Acampora D., Avantaggiato V., Tuorto F., Briata P., Corte G. and Simeone A. (1998) Visceral endoderm-restricted translation of Otx1 mediates recovery of Otx2 requirements for specification of anterior neural plate and normal gastrulation. *Development* **125**, 5091–5104.

Bird A. P. and Wolffe A. P. (1999) Methylation-induced repression – belts, braces, and chromatin. *Cell* **99**, 451–454.

Bonni A., Sun Y., Nadal-Vicens M., Bhatt A., Frank D. A., Rozovsky I., Stahl N., Yancopoulos G. D. and Greenberg M. E. (1997) Regulation of gliogenesis in the central nervous system by the JAK-STAT signaling pathway. *Science* **278**, 477–483.

Bradley A., Evans M., Kaufman M. H. and Robertson E. (1984) Formation of germ-line chimaeras from embryo-derived teratocarcinoma cell lines. *Nature* **309**, 255–256.

Clark S. J., Harrison J., Paul C. L. and Frommer M. (1994) High sensitivity mapping of methylated cytosines. *Nucl. Acids Res.* **22**, 2990–2997.

Doetschman T. C., Eistetter H., Katz M., Schmidt W. and Kemler R. (1985) The in vitro development of blastocyst-derived embryonic stem cell lines: formation of visceral yolk sac, blood islands and myocardium. *J. Embryol. Exp. Morph.* **87**, 27–45.

Dziadek M. and Adamson E. (1978) Localization and synthesis of alphafoetoprotein in post-implantation mouse embryos. *J. Embryol. Exp. Morph.* **43**, 289–313.

Gage F. H. (2000) Mammalian neural stem cells. *Science* **287**, 1433–1438.

Jaenisch R. (1997) DNA methylation and imprinting: why bother? *Trends Genet.* **13**, 323–329.

Kawasaki H., Mizuseki K., Nishikawa S., Kaneko S., Kuwana Y., Nakanishi S., Nishikawa S. I. and Sasai Y. (2000) Induction of midbrain dopaminergic neurons from ES cells by stromal cell-derived inducing activity. *Neuron* **28**, 31–40.

Lunyak V. V., Burgess R., Prefontaine G. G. *et al.* (2002) Corepressor-dependent silencing of chromosomal regions encoding neuronal genes. *Science* **298**, 1747–1752.

Ma Q., Sommer L., Cserjesi P. and Anderson D. J. (1997) Mash1 and neurogenin1 expression patterns define complementary domains of neuroepithelium in the developing CNS and are correlated with regions expressing notch ligands. *J. Neurosci.* **17**, 3644–3652.

McGowan K. M. and Coulombe P. A. (1998) Onset of keratin 17 expression coincides with the definition of major epithelial lineages during skin development. *J. Cell Biol.* **143**, 469–486.

McKay R. (1997) Stem cells in the central nervous system. *Science* **276**, 66–71.

Nakashima K., Yanagisawa M., Arakawa H. and Taga T. (1999a) Astrocyte differentiation mediated by LIF in cooperation with BMP2. *FEBS Lett.* **457**, 43–46.

Nakashima K., Yanagisawa M., Arakawa H., Kimura N., Hisatsune T., Kawabata M., Miyazono K. and Taga T. (1999b) Synergistic signaling in fetal brain by STAT3-Smad1 complex bridged by p300. *Science* **284**, 479–482.

Nakashima K., Wiese S., Yanagisawa M., Arakawa H., Kimura N., Hisatsune T., Yoshida K., Kishimoto T., Sendtner M. and Taga T. (1999c) Developmental requirement of gp130 signaling in neuronal survival and astrocyte differentiation. *J. Neurosci.* **19**, 5429–5434.

Qian X., Shen Q., Goderie S. K., He W., Capela A., Davis A. A. and Temple S. (2000) Timing of CNS cell generation: a programmed sequence of neuron and glial cell production from isolated murine cortical stem cells. *Neuron* **28**, 69–80.

Rajan P. and McKay R. D. (1998) Multiple routes to astrocytic differentiation in the CNS. *J. Neurosci.* **18**, 3620–3629.

Shimozaki K., Nakashima K., Niwa H. and Taga T. (2003) Involvement of Oct3/4 in the enhancement of neuronal differentiation of ES cells in neurogenesis-inducing cultures. *Development* **130**, 2505–2512.

Simeone A., Gulisano M., Acampora D., Stornaiuolo A., Rambaldi M. and Boncinelli E. (1992) Two vertebrate homeobox genes related to the Drosophila empty spiracles gene are expressed in the embryonic cerebral cortex. *EMBO J.* **11**, 2541–2550.

Stewart C. L., Stuhlmann H., Jahner D. and Jaenisch R. (1982) De novo methylation, expression, and infectivity of retroviral genomes introduced into embryonal carcinoma cells. *Proc. Natl Acad. Sci. USA* **79**, 4098–4102.

Takizawa T., Nakashima K., Namihira M., Ochiai W., Uemura A., Yanagisawa M., Fujita N., Nakao M. and Taga T. (2001) DNA methylation is a critical cell-intrinsic determinant of astrocyte differentiation in the fetal brain. *Dev. Cell* **1**, 749–758.

Teter B., Rozovsky I., Krohn K., Anderson C., Osterburg H. and Finch C. (1996) Methylation of the glial fibrillary acidic protein gene shows novel biphasic changes during brain development. *Glia* **17**, 195–205.

Wilkinson D. G., Bhatt S. and Herrmann B. G. (1990) Expression pattern of the mouse T gene and its role in mesoderm formation. *Nature* **343**, 657–659.

Immunity 24, 41–51, January 2006 ©2006 Elsevier Inc. DOI 10.1016/j.immuni.2005.11.004

IκBNS Inhibits Induction of a Subset of Toll-like Receptor-Dependent Genes and Limits Inflammation

Hirotaka Kuwata,[1] Makoto Matsumoto,[1] Koji Atarashi,[1] Hideaki Morishita,[1] Tomohiro Hirotani,[2] Ritsuko Koga,[1] and Kiyoshi Takeda[1,*]
[1] Department of Molecular Genetics
Medical Institute of Bioregulation
Kyushu University
3-1-1 Maidashi, Higashi-ku
Fukuoka 812-8582
Japan
[2] Department of Gastroenterology and Hepatology
Graduate School of Medicine
Osaka University
2-2 Yamada-oka, Suita
Osaka 565-0871
Japan

Summary

Toll-like receptor (TLR)-mediated immune responses are downregulated by several mechanisms that affect signaling pathways. However, it remains elusive how TLR-mediated gene expression is differentially modulated. Here, we show that IκBNS, a TLR-inducible nuclear IκB protein, negatively regulates induction of a subset of TLR-dependent genes through inhibition of NF-κB activity. IκBNS-deficient macrophages and dendritic cells show increased TLR-mediated expression of genes such as IL-6 and IL-12p40, which are induced late after TLR stimulation. In contrast, IκBNS-deficient cells showed normal induction of genes that are induced early or induced via IRF-3 activation. LPS stimulation of IκBNS-deficient macrophages prolonged NF-κB activity at the specific promoters, indicating that IκBNS mediates termination of NF-κB activity at selective gene promoters. Moreover, IκBNS-deficient mice are highly susceptible to LPS-induced endotoxin shock and intestinal inflammation. Thus, IκBNS regulates inflammatory responses by inhibiting the induction of a subset of TLR-dependent genes through modulation of NF-κB activity.

Introduction

Toll-like receptors (TLRs) are implicated in the recognition of specific patterns of microbial components and subsequent induction of gene expression. TLR-dependent gene expression is induced through activation of two distinct signaling pathways mediated by the Toll/IL-1 receptor (TIR) domain-containing adaptors MyD88 and TRIF. These signaling pathways finally culminate in the activation of several transcription factors, such as NF-κB and IRF families (Akira and Takeda, 2004). The MyD88-dependent gene induction is achieved by an early phase of NF-κB and IRF-5 activation in macrophages (Kawai et al., 1999; Takaoka et al., 2005). The TRIF-dependent gene induction is mainly regulated by IRF-3 (Sakaguchi et al., 2003; Yamamoto et al., 2003).

TLR-mediated gene expression regulates activation of not only innate immunity but also adaptive immunity, which provides antigen-specific responses against harmful pathogens (Iwasaki and Medzhitov, 2004; Pasare and Medzhitov, 2004). However, TLR-mediated activation of innate immunity, when in excess, triggers development of autoimmune disorders and inflammatory diseases, such as SLE, cardiomyopathy, atherosclerosis, diabetes mellitus, and inflammatory bowel diseases (Bjorkbacka et al., 2004; Eriksson et al., 2003; Kobayashi et al., 2003; Lang et al., 2005; Leadbetter et al., 2002; Michelsen et al., 2004). Excessive activation of TLR4 by LPS induces endotoxin shock, a serious systemic disorder with a high mortality rate. Therefore, TLR-dependent innate immune responses must be finely regulated, and underlying mechanisms are now being examined extensively (Liew et al., 2005). Several negative regulators of TLR-mediated signaling pathways have been proposed. Cytoplasmic molecules, such as an alternatively spliced short form of MyD88 (MyD88s), IRAK-M, SOCS1, A20, PI3-kinase, and TRIAD3A, are all involved in negative regulation of TLR pathways (Boone et al., 2004; Burns et al., 2003; Chuang and Ulevitch, 2004; Fukao et al., 2002; Kinjyo et al., 2002; Kobayashi et al., 2002; Nakagawa et al., 2002). Membrane bound SIGIRR, ST2, TRAILR, and RP105 are also implicated in these processes (Brint et al., 2004; Diehl et al., 2004; Divanovic et al., 2005; Wald et al., 2003).

TLR-dependent gene induction is also regulated by nuclear IκB proteins, such as IκBζ, Bcl-3, and IκBNS. IκBζ is indispensable for positive regulation of a subset of TLR-dependent genes, such as IL-6 and IL-12p40 (Yamamoto et al., 2004). In contrast, Bcl-3 and IκBNS seem to be involved in negative regulation of TLR-dependent gene induction. Bcl-3 was shown to be involved in selective inhibition of TLR-dependent TNF-α production (Kuwata et al., 2003; Wessells et al., 2004). An in vitro study indicated that IκBNS is induced by IL-10 or LPS and selectively inhibits IL-6 production in macrophages (Hirotani et al., 2005). Thus, nuclear IκB proteins differentially regulate TLR-dependent gene expression. However, the physiological role of IκBNS is still unclear.

In this study, we analyzed TLR-dependent inflammatory responses in IκBNS-deficient mice. We found that IκBNS is involved in selective inhibition of a subset of MyD88-dependent genes, including IL-6, IL-12p40, and IL-18. In IκBNS-deficient macrophages, LPS-induced activation of NF-κB was prolonged. Accordingly, IκBNS-deficient mice showed increased production of these cytokines accompanied by high sensitivity to LPS-induced endotoxin shock. Furthermore, IκBNS-deficient mice were highly susceptible to intestinal inflammation caused by disruption of the epithelial barrier. These findings indicate that IκBNS inhibits the induction of a group of TLR-dependent genes, thereby preventing excessive inflammation.

*Correspondence: ktakeda@bioreg.kyushu-u.ac.jp

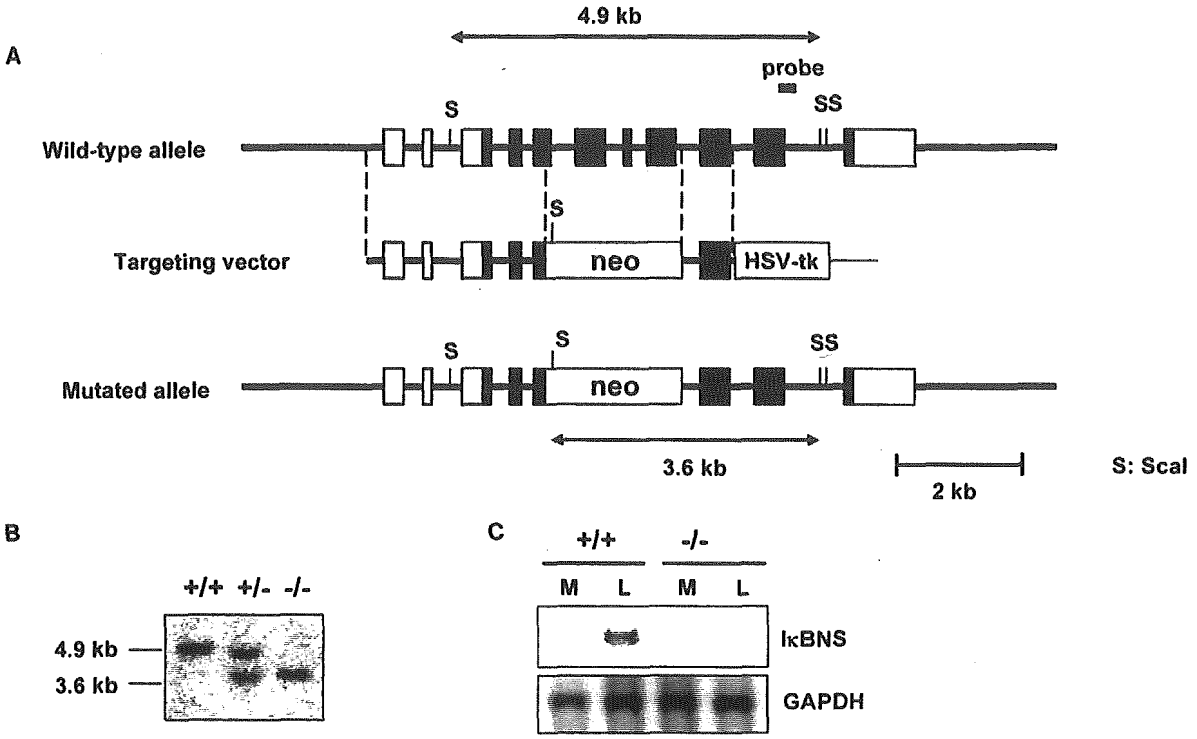

Figure 1. Targeted Disruption of the Mouse *Ikbns* Gene

(A) Maps of the IκBNS wild-type genome, targeting vector, and predicted targeted gene. Open and closed boxes denote the noncoding and coding exons, respectively. Restriction enzymes: S, ScaI.

(B) Southern blot analysis of offspring from the heterozygote intercrosses. Genomic DNA was extracted from mouse tails, digested with ScaI, electrophoresed, and hybridized with the probe indicated in (A). The approximate size of the wild-type band is 4.9 kb, and the mutated band is 3.6 kb.

(C) Peritoneal macrophages were cultured with or without 100 ng/ml LPS for 1 hr (L and M, respectively), and total RNA was extracted, electrophoresed, transferred to nylon membrane, and hybridized with the mouse IκBNS full-length cDNA probe. The same membrane was rehybridized with a GAPDH probe.

Results

Targeted Disruption of the IκBNS Gene

To study the functional role of IκBNS in TLR-dependent responses, a null mutation in the *Ikbns* allele was introduced through homologous recombination in embryonic stem (ES) cells (Figures 1A and 1B). IκBNS$^{-/-}$ mice were born alive and grew healthy until 20 weeks of age. We performed Northern blot analysis to confirm that the mutation causes inactivation of the *Ikbns* gene. LPS robustly induced IκBNS mRNA in wild-type macrophages, but not in IκBNS$^{-/-}$ macrophages (Figure 1C).

A previous report indicated that IκBNS is involved in negative selection of thymocytes (Fiorini et al., 2002). Therefore, we first analyzed lymphocyte composition in lymphoid organs such as thymus and spleen by flow cytometry (Figures S1A and S1B). Total cell number and CD4/CD8 or CD3/B220 populations in thymus and spleen were not altered in IκBNS$^{-/-}$ mice. Splenic T cells from IκBNS$^{-/-}$ mice showed similar levels of proliferative responses to IL-2 and IL-7 as did wild-type T cells. Moreover, IκBNS$^{-/-}$ T cells proliferated to almost equal degrees in response to anti-CD3 antibody compared to wild-type T cells (Figure S1C). These results indicate that T cell development and functions were generally unaffected in IκBNS$^{-/-}$ mice.

Increased IL-6 and IL-12p40 Production in IκBNS-Deficient Cells

Since IκBNS expression was induced within 1 hr of LPS stimulation in macrophages (Figure 1B), we stimulated peritoneal macrophages with various concentrations of LPS and analyzed for production of TNF-α and IL-6 (Figure 2A). In macrophages from IκBNS$^{-/-}$ mice, LPS-induced TNF-α production was comparable to wild-type cells, but IL-6 production was significantly increased. We then analyzed whether IκBNS$^{-/-}$ macrophages produce increased amounts of IL-6 in response to other TLR ligands, since IκBNS mRNA was induced by several TLR ligands as well as the TLR4 ligand LPS in a MyD88-dependent manner (Figure S2A). Peritoneal macrophages were stimulated with mycoplasmal lipopeptides (TLR6 ligand), Pam_3CSK_4 (TLR1 ligand), peptidoglycan (TLR2 ligand), and imiquimod (TLR7 ligand), and analyzed for production of TNF-α and IL-6 (Figure 2B). In response to these TLR ligands, the production of IL-6, but not TNF-α, was increased in IκBNS$^{-/-}$ mice. We next analyzed the response of bone marrow-derived dendritic cells (DCs). DCs from IκBNS$^{-/-}$ mice produced similar amounts of TNF-α and increased amounts of IL-6 in response to LPS compared to wild-type DCs (Figure 2C). In addition, DCs showed LPS-induced production of IL-12p40 and IL-12p70, and production of these

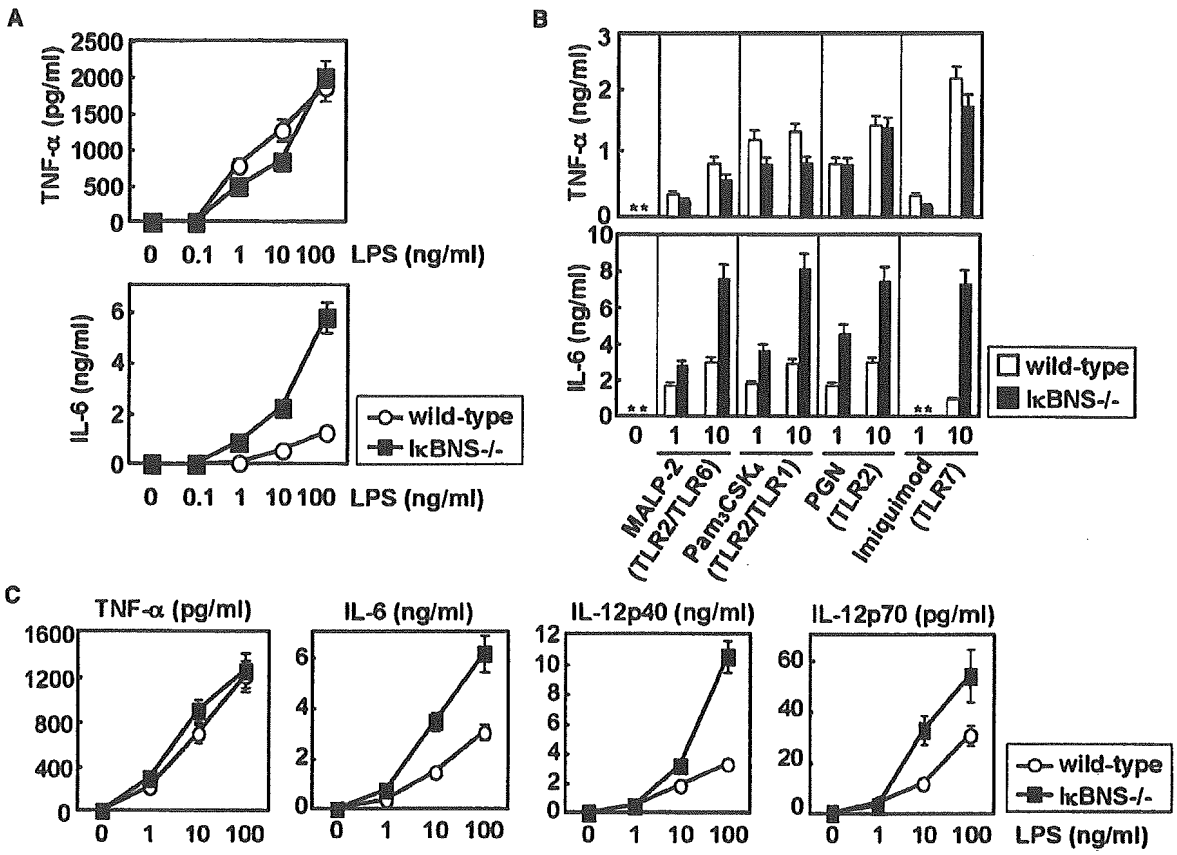

Figure 2. Increased Production of IL-6 and IL-12p40 in IκBNS$^{-/-}$ Macrophages and Dendritic Cells

(A) Peritoneal macrophages were stimulated with the indicated concentration of LPS for 24 hr. Concentrations of TNF-α and IL-6 in the culture supernatants were analyzed by ELISA. Data are mean ± SD of triplicate cultures in a single experiment, representative of three independent experiments.

(B) Peritoneal macrophages were cultured with 1 or 10 ng/ml of TLR6 ligand (MALP-2), 1 or 10 ng/ml TLR1 ligand (Pam_3CSK_4), 1 or 10 μg/ml TLR2 ligand (peptidoglycan; PGN), or 1 or 10 μg/ml TLR7 ligand (imiquimod) for 24 hr. Concentrations of TNF-α and IL-6 in the culture supernatants were analyzed by ELISA. *; not detected.

(C) Bone marrow-derived DCs were stimulated with the indicated concentration of LPS for 24 hr. Concentrations of TNF-α, IL-6, IL-12p40, and IL-12p70 in the culture supernatants were analyzed by ELISA. Data are mean ± SD of triplicate cultures in a single experiment, representative of three independent experiments.

cytokines was significantly increased in IκBNS$^{-/-}$ DCs. Bone marrow-derived DCs and splenic B cells were analyzed for LPS-induced surface expression of CD86 or MHC class II (Figure S2B). LPS-induced augmentation of surface expression of these molecules was not altered in IκBNS$^{-/-}$ mice. Thus, macrophages and DCs from IκBNS$^{-/-}$ mice showed selective increases in TLR-dependent production of IL-6 and IL-12p40.

Enhanced Induction of a Subset of TLR-Dependent Genes in IκBNS-Deficient Macrophages

We further analyzed LPS-induced mRNA expression of TLR-dependent genes in IκBNS$^{-/-}$ macrophages. Peritoneal macrophages were stimulated with LPS for 1, 3, or 5 hr, and total RNA was extracted. Then, mRNA expression of TNF-α and IL-6 was first analyzed by quantitative real-time RT-PCR (Figures 3A and 3B). LPS-induced TNF-α mRNA expression in IκBNS$^{-/-}$ macrophages was similar to wild-type cells. In the case of IL-6 mRNA, expression levels were comparable between wild-type and IκBNS$^{-/-}$ macrophages until 3 hr of LPS stimulation. After 3 hr, IL-6 mRNA levels decreased in wild-type cells. However, IκBNS$^{-/-}$ cells displayed further enhanced expression of IL-6 mRNA. TNF-α mRNA was robustly induced within 1 hr of LPS stimulation, and its expression promptly ceased in wild-type cells. In contrast, IL-6 mRNA expression was induced late compared to TNF-α. Because LPS-induced IκBNS mRNA expression showed similar patterns as TNF-α mRNA, we hypothesized that LPS-inducible IκBNS blocks mRNA expression of genes that are induced late (Figure 3C). Accordingly, we analyzed mRNA expression of other genes that are induced early (*Il-1β*, *Il-23p19*, or *Ikbz*) or late (*Il-12p40*, *Il-18*, or *Csf3*) in response to LPS. LPS-induced mRNA expression of *Il-1β* (IL-1β), *Il-23p19* (IL-23p19), and *Ikbz* (IκBζ) was similarly observed between wild-type and IκBNS$^{-/-}$ macrophages (Figure 3A). LPS-induced expression of *Il-12p40* (IL-12p40), *Il-18* (IL-18) and *Csf3* (G-CSF) was observed at normal levels in IκBNS$^{-/-}$ macrophages at the early phase of LPS stimulation (within 3 hr of LPS stimulation) (Figure 3B). However, at the late phase of LPS stimulation (after 3 hr of LPS stimulation), mRNA expression of these genes was significantly enhanced in

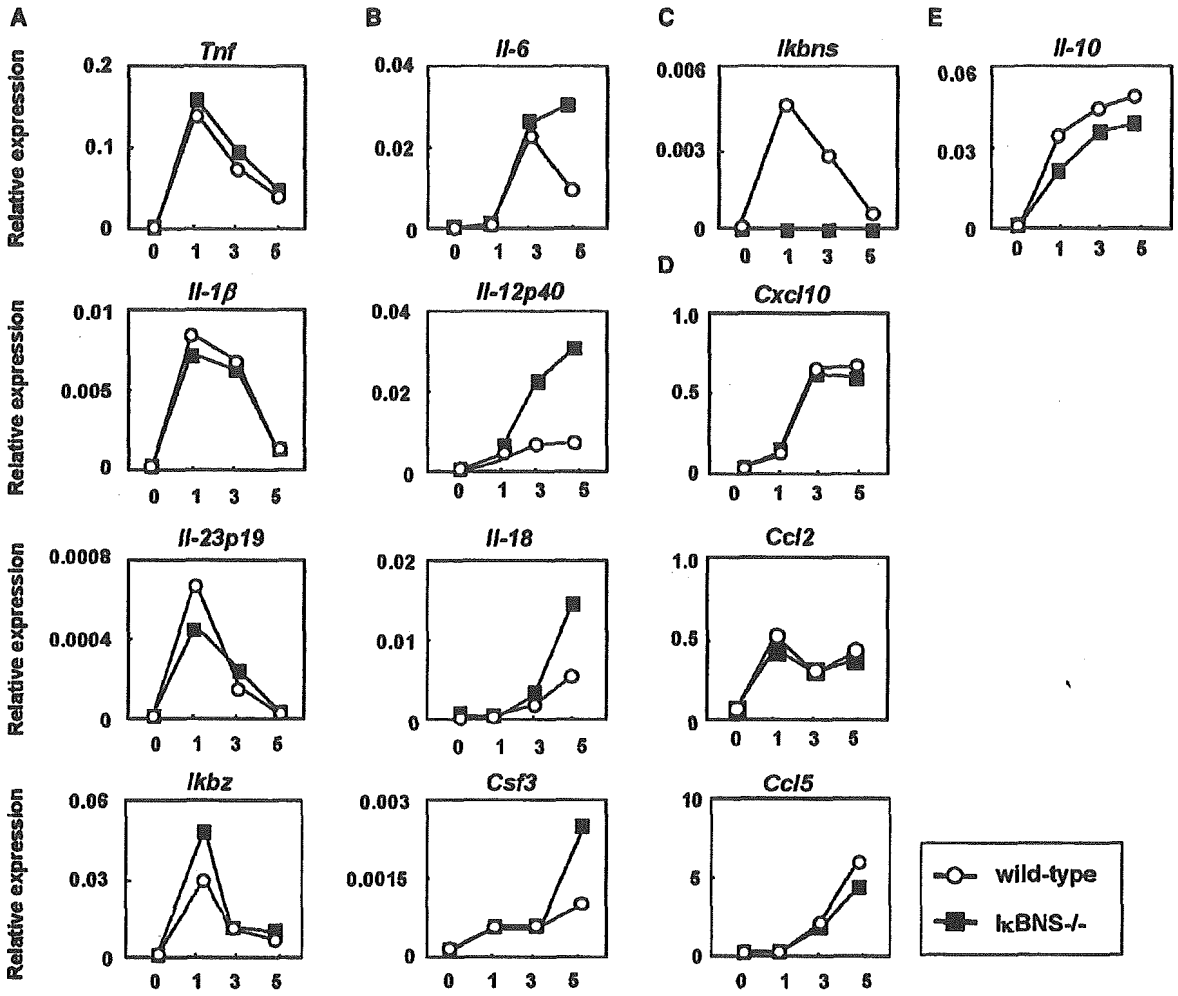

Figure 3. LPS-Induced Expression of Several TLR-Dependent Genes in IκBNS$^{-/-}$ Macrophages

Peritoneal macrophages from wild-type and IκBNS$^{-/-}$ mice were stimulated with 100 ng/ml LPS for the indicated periods. Total RNA was extracted, and then subjected to quantitative real-time RT-PCR analysis using primers specific for *Tnf*, *Il-1β*, *Il-23p19*, *Ikbz* (A), *Il-6*, *Il-12p40*, *Il-18*, *Csf3* (B), *Ikbns* (C), *Cxcl10*, *Ccl2*, *Ccl5* (D), and *Il-10* (E). The fold difference of each sample relative to EF-1α levels is shown. Representative of three independent experiments.

IκBNS$^{-/-}$ cells. We also analyzed LPS-induced expression of *Cxcl10* (IP-10), *Ccl2* (MCP-1), and *Ccl5* (RANTES), which are induced by the TRIF-dependent activation of IRF-3 (Figure 3D). LPS-induced expression of these genes was not altered in IκBNS$^{-/-}$ macrophages. An anti-inflammatory cytokine IL-10 is induced by TLR stimulation and thereby inhibits TLR-dependent gene induction (Moore et al., 2001). Therefore, we next addressed LPS-induced IL-10 mRNA expression (Figure 3E). LPS-induced IL-10 mRNA expression was comparable between wild-type and IκBNS$^{-/-}$ macrophages. In addition, LPS-induced production of IL-10 protein was not compromised in IκBNS$^{-/-}$ DCs (Figure S2C). These findings indicate that the enhanced LPS-induced expression of a subset of TLR-dependent genes was not due to the impaired IL-10 production in IκBNS$^{-/-}$ mice.

Prolonged NF-κB Activity in IκBNS-Deficient Cells

Gene expression of *Cxcl10* (IP-10), *Ccl2* (MCP-1), and *Ccl5* (RANTES) was mainly regulated by the transcription factor IRF-3 in the TRIF-dependent pathway, whereas TNF-α, IL-6, and IL-12p40 gene expression was mainly regulated by the MyD88-dependent activation of NF-κB (Akira and Takeda, 2004; Yamamoto et al., 2003). In addition, previous in vitro studies indicated that overexpression of IκBNS leads to compromised NF-κB activity through selective association of IκBNS with p50 subunit of NF-κB (Fiorini et al., 2002; Hirotani et al., 2005). Therefore, we next analyzed LPS-induced activation of NF-κB. LPS-induced degradation of IκBα was not compromised in IκBNS$^{-/-}$ macrophages (Figure S3A). Next, peritoneal macrophages or bone marrow-derived macrophages were stimulated with LPS and DNA binding activity was analyzed by EMSA (Figure 4A; Figure S3B). LPS stimulation resulted in enhanced DNA binding activity of NF-κB in both wild-type and IκBNS$^{-/-}$ macrophages to similar extents within 1 hr. After 1 hr of LPS stimulation, NF-κB activity decreased in wild-type cells. However, NF-κB activity sustained and even at 3 hr of LPS stimulation significant DNA binding activity was still observed in

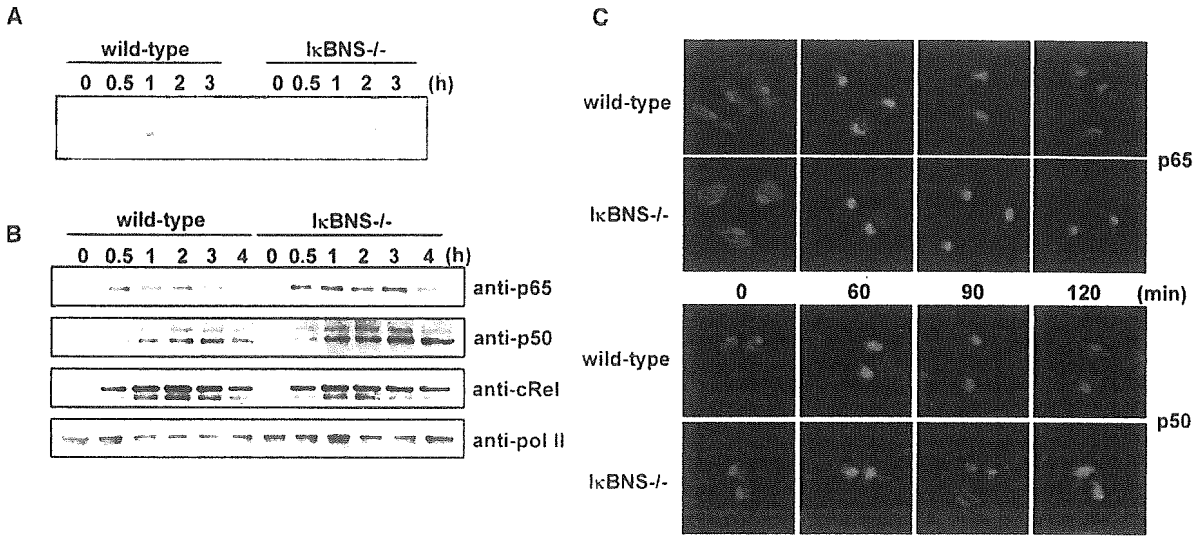

Figure 4. Persistent LPS-Induced Activation of NF-κB in IκBNS$^{-/-}$ Macrophages

(A) Peritoneal macrophages from wild-type and IκBNS$^{-/-}$ mice were stimulated with 100 ng/ml LPS. At the indicated time points, nuclear extracts were prepared, and NF-κB activation was analyzed by EMSA using a NF-κB specific probe.

(B) Peritoneal macrophages were stimulated with LPS. At the indicated time points, nuclear fractions were isolated and subjected to Western blotting using anti-p65 Ab, anti-p50 Ab, anti-cRel Ab, or anti-polII Ab.

(C) Macrophages were stimulated with LPS for the indicated periods. Then, cells were stained with anti-p65 Ab or anti-p50 Ab (red) as well as DAPI (blue), and analyzed by confocal microscopy. Merged images are shown.

IκBNS$^{-/-}$ cells. We next analyzed nuclear localization of NF-κB subunits. Peritoneal macrophages were stimulated with LPS for the indicated periods, and nuclear fractions were analyzed for expression of p65, p50, and c-Rel by immunoblotting (Figure 4B). In wild-type macrophages, nuclear translocation of p65 was observed within 30 min of LPS stimulation, and nuclear localized p65 gradually decreased thereafter. In contrast, nuclear localized p65 was still significantly observed even at 3 hr of LPS stimulation in IκBNS$^{-/-}$ cells. In addition, sustained nuclear localization of p50, but not c-Rel, was observed in IκBNS$^{-/-}$ macrophages (Figure 4B). Nuclear localization of NF-κB subunits was also analyzed by immunofluorescent staining of macrophages (Figure 4C). Without stimulation, p65 and p50 were localized in the cytoplasm, but not in the nucleus, in both wild-type and IκBNS$^{-/-}$ macrophages. LPS stimulation resulted in nuclear staining of both p65 and p50 at 1 hr. Nuclear staining of p65 and p50 gradually decreased after 1 hr of LPS stimulation and was only faintly observed at 2 hr of stimulation in wild-type cells. However, nuclear localization of p65 and p50 was still evident at 2 hr of LPS stimulation in IκBNS$^{-/-}$ cells. These findings indicate that LPS-induced NF-κB activity was prolonged in IκBNS$^{-/-}$ macrophages. NF-κB activity is terminated by degradation of promoter-bound p65 (Natoli et al., 2005; Saccani et al., 2004). We used RAW264.7 macrophage cell line and performed pulse-chase experiments with ^{35}S-labeled amino acids to analyze p65 turnover (Figure S3C). In these cells, labeled p65 was accumulated into the nucleus until 2 hr of LPS stimulation, and then p65 was degraded. In RAW cells constitutively expressing IκBNS, nuclear accumulation of labeled p65 was similarly observed until 1 hr of LPS stimulation. However, the p65 turnover was observed more rapidly and labeled p65 disappeared at 2 hr after LPS stimulation (Figure S3C). These findings indicate that IκBNS mediates the degradation of p65. The MyD88-dependent pathway mediates activation of MAP kinase cascades as well as NF-κB activation. Therefore, LPS-induced phosphorylation of p38, ERK1, ERK2, and JNK was analyzed by Western blotting (Figure S3D). LPS-induced activation of these MAP kinases was not compromised in IκBNS$^{-/-}$ macrophages.

Regulation of p65 Activity at the IL-6 Promoter by IκBNS

We next addressed how IκBNS selectively downregulates induction of genes that are induced late. We utilized the IL-6 and TNF-α promoters, which are representatives of genes activated late and early, respectively. Wild-type macrophages were stimulated with LPS and analyzed for recruitment of endogenous IκBNS to the promoters by chromatin immunoprecipitation (ChIP) assay (Figure 5A). Consistent with previous findings using IκBNS overexpressing macrophage cell lines (Hirotani et al., 2005), endogenous IκBNS was recruited to the IL-6 promoter, but not the TNF-α promoter, in LPS-stimulated macrophages. We next addressed LPS-induced recruitment of p65 to the promoters in wild-type and IκBNS$^{-/-}$ macrophages (Figure 5B). Recruitment of p65 to the TNF-α promoter peaked at 1 hr of LPS stimulation and gradually decreased thereafter in a similar manner in both wild-type and IκBNS$^{-/-}$ cells. Recruitment of p65 to the IL-6 promoter was observed to similar extents until 3 hr of LPS stimulation in wild-type and IκBNS$^{-/-}$ macrophages. After that, it decreased in wild-type macrophages. In contrast, p65 recruitment was still evident, rather enhanced, even after 5 hr of LPS stimulation in IκBNS$^{-/-}$ macrophages. Thus, p65 activity at

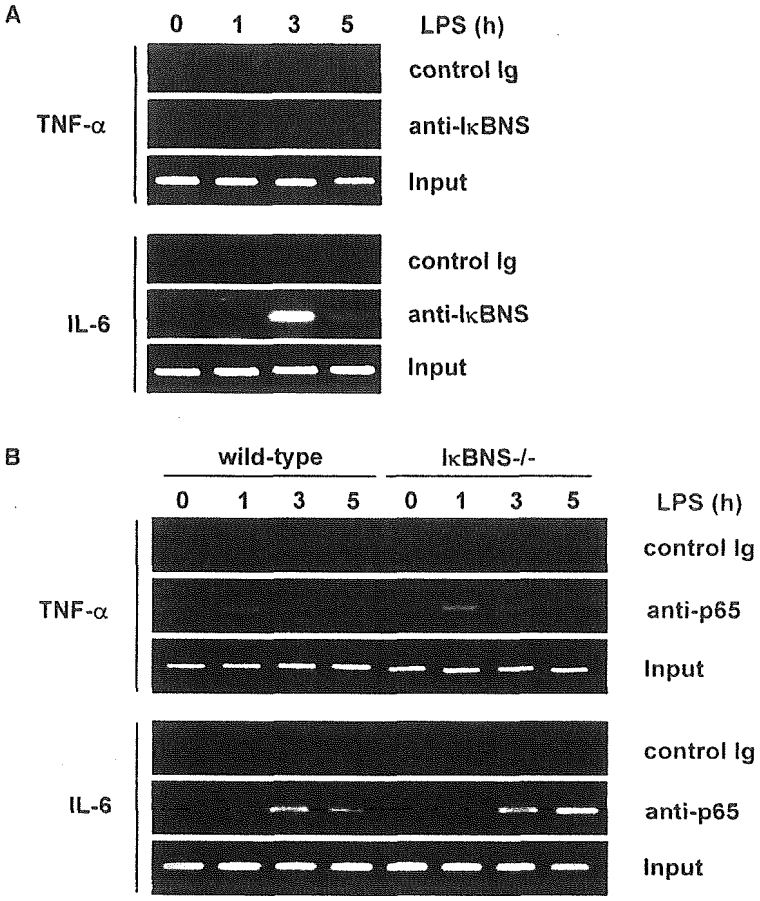

Figure 5. IκBNS Regulation of p65 Activity at the IL-6 Promoter

(A) Wild-type bone marrow-derived macrophages were stimulated with 100 ng/ml of LPS for the indicated periods, and chromatin immunoprecipitation (ChIP) assay was performed with anti-IκBNS Ab or control Ig. The immunoprecipitated TNF-α promoter (upper panel) or IL-6 promoter (lower panel) was analyzed by PCR with promoter-specific primers. PCR amplification of the total input DNA in each sample is shown (Input). Representative of three independent experiments. The same result was obtained when peritoneal macrophages were used.

(B) Macrophages from wild-type or IκBNS$^{-/-}$ mice were stimulated with LPS for the indicated periods. Then, ChIP assay was performed with anti-p65 Ab or control Ig. The immunoprecipitated TNF-α promoter (upper panel) or IL-6 promoter (lower panel) was analyzed by PCR with promoter-specific primers. Representative of three independent experiments.

the IL-6 promoter, but not at the TNF-α promoter, was prolonged in LPS-stimulated IκBNS$^{-/-}$ macrophages. Taken together, these findings indicate that TLR-inducible IκBNS is responsible for termination of NF-κB activity through its recruitment to specific promoters.

High Sensitivity to LPS-Induced Endotoxin Shock in IκBNS-Deficient Mice

To study the in vivo role of IκBNS, we examined LPS-induced endotoxin shock. Intraperitoneal injection of LPS resulted in marked increases in serum concentrations of TNF-α, IL-6, and IL-12p40 (Figure 6A). TNF-α level was comparable between wild-type and IκBNS$^{-/-}$ mice, which rapidly peaked at around 1.5 hr of LPS administration. In the case of IL-6 and IL-12p40 levels, concentrations of both cytokines were almost equally elevated within 3 hr of LPS injection. After 3 hr, levels of both cytokines gradually decreased in wild-type mice. However, concentrations of IL-6 and IL-12p40 sustained, rather enhanced, in IκBNS$^{-/-}$ mice after 3 hr. Thus, persistently high concentrations of LPS-induced serum IL-6 and IL-12p40 were observed in IκBNS$^{-/-}$ mice. Furthermore, high sensitivity to LPS-induced lethality was observed in IκBNS$^{-/-}$ mice (Figure 6B). All IκBNS$^{-/-}$ mice died within 4 days of LPS challenge at a dose of which almost all wild-type mice survived over 4 days. These findings indicate that IκBNS$^{-/-}$ mice are highly sensitive to LPS-induced endotoxin shock.

High Susceptibility to DSS-Induced Colitis in IκBNS$^{-/-}$ Mice

In a previous report, IκBNS was shown to be constitutively expressed in macrophages residing in the colonic lamina propria, which explains one of the mechanisms for hyporesponsiveness to TLR stimulation in these cells (Hirotani et al., 2005). Therefore, we next stimulated CD11b^{+} cells isolated from the colonic lamina propria with LPS and analyzed for production of TNF-α and IL-6 (Figure S4). In CD11b^{+} cells from wild-type mice, LPS-induced production of these cytokines was not significantly observed. In cells from IκBNS$^{-/-}$ mice, IL-6 production was increased even in the absence of stimulation, and LPS stimulation led to markedly enhanced production of IL-6, but not TNF-α. In the next experiment, in order to expose these cells to microflora and cause intestinal inflammation, mice were orally administered with dextran sodium sulfate (DSS), which is toxic to colonic epithelial cells and therefore disrupts the epithelial cell barrier (Kitajima et al., 1999). IκBNS$^{-/-}$ mice showed more severe weight loss compared with wild-type mice (Figure 7A). Histological analyses of the colon indicated that the inflammatory lesions were more severe and more extensive in IκBNS$^{-/-}$ mice (Figures 7B and 7C). Thus, IκBNS$^{-/-}$ mice are highly susceptible to intestinal inflammation. Th1-oriented CD4^{+} T cell response was shown to be associated with DSS colitis (Strober et al., 2002). Therefore, we analyzed IFN-γ

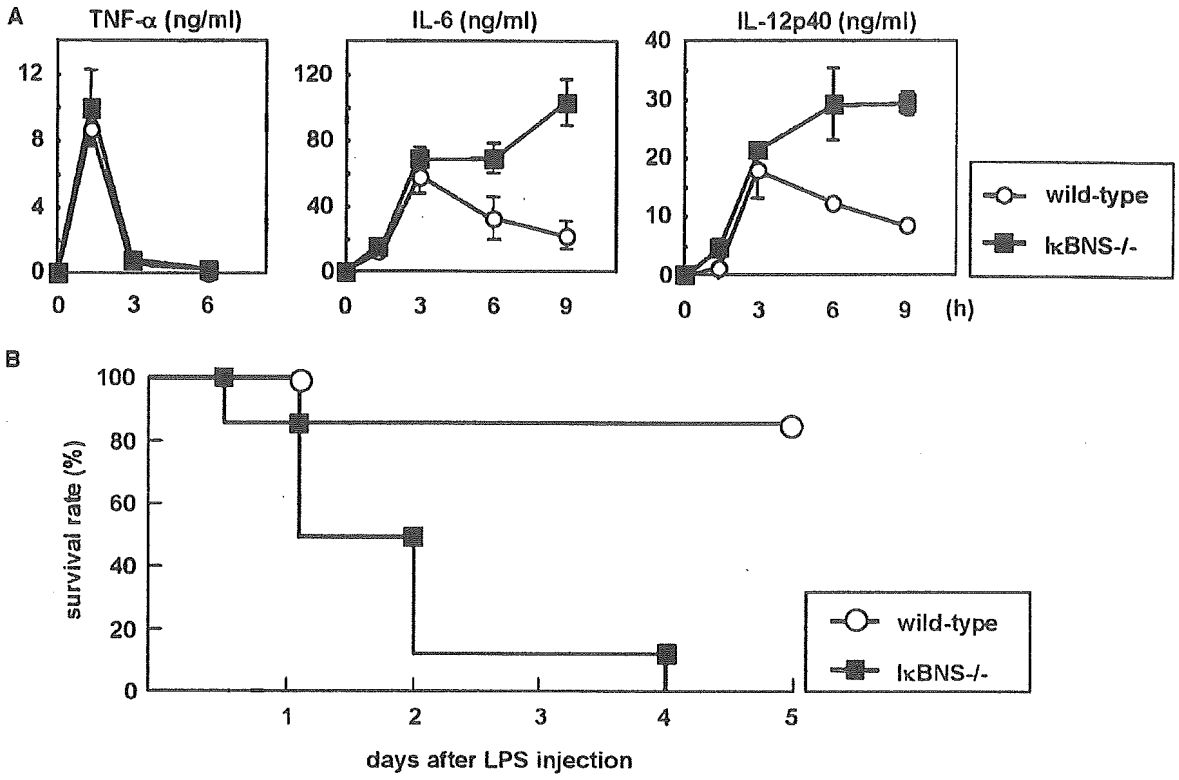

Figure 6. High Susceptibility to LPS-Induced Endotoxin Shock in IκBNS$^{-/-}$ Mice

Age-matched wild-type (n = 6) and IκBNS−/− (n = 6) mice were intraperitoneally injected with LPS (1 mg). (A) Sera were taken at 1.5, 3, 6, and 9 hr after LPS injection. Serum concentrations of TNF-α, IL-6, and IL-12p40 were determined by ELISA. Results are shown as mean ± SD of serum samples from six mice. (B) Survival was monitored for 5 days.

production from splenic CD4$^+$ T cells of wild-type and IκBNS$^{-/-}$ mice before and after DSS administration (Figure 7D). DSS administration led to a mild increase in IFN-γ production in wild-type mice. In nontreated IκBNS$^{-/-}$ mice, IFN-γ production was slightly increased compared with nontreated wild-type mice. In DSS-fed IκBNS$^{-/-}$ mice, a significant increase in IFN-γ production was observed compared to DSS-fed wild-type mice. These results indicate that IκBNS$^{-/-}$ mice are susceptible to intestinal inflammation caused by exposure to microflora.

Discussion

In the present study, we characterized the physiological function of IκBNS. Induced by TLR stimulation, IκBNS is involved in termination of NF-κB activity and thereby inhibits a subset of TLR-dependent genes that are induced late through MyD88-dependent NF-κB activation. Accordingly, IκBNS$^{-/-}$ mice show sustained production of IL-6 and IL-12p40, resulting in high susceptibility to LPS-induced endotoxin shock. Furthermore, IκBNS$^{-/-}$ mice are susceptible to intestinal inflammation accompanied by enhanced Th1 responses.

IκBNS was originally identified as a molecule that mediates negative selection of thymocytes (Fiorini et al., 2002). However, IκBNS$^{-/-}$ mice did not show any defect in T cell development. Requirement of IκBNS in negative selection of thymocytes should be analyzed precisely using peptide-specific TCR transgenic mice, such as mice bearing the H-Y TCR, in the future (Kisielow et al., 1988).

Recent studies have established that TLR-dependent gene induction is regulated mainly by NF-κB and IRF families of transcription factors (Akira and Takeda, 2004; Honda et al., 2005; Takaoka et al., 2005). In TLR4 signaling, the TRIF-dependent pathway is responsible for induction of IFN-β and IFN-inducible genes through activation of IRF-3, whereas the MyD88-dependent pathway mediates induction of several NF-κB dependent genes (Beutler, 2004). A study with mice lacking IκBζ, another member of nuclear IκB proteins, has demonstrated that the MyD88-dependent genes are divided into at least two types; one is induced early and independent of IκBζ, and another is induced late and dependent on IκBζ (Yamamoto et al., 2004). The IκBζ-regulated genes include IL-6, IL-12p40, IL-18, and G-CSF, which are all upregulated in LPS-stimulated IκBNS$^{-/-}$ macrophages. Thus, IκBNS seems to possess a function quite opposite to IκBζ. IκBNS is most structurally related to IκBζ (Fiorini et al., 2002; Hirotani et al., 2005). But, IκBζ has an additional N-terminal structure, which seemingly mediates the induction of target genes (Motoyama et al., 2005). Thus, nuclear IκB proteins IκBζ and IκBNS positively and negatively regulate a subset of TLR-induced NF-κB-dependent genes, respectively.

Recently, negative regulation of TLR-dependent gene induction was extensively analyzed (Liew et al., 2005).

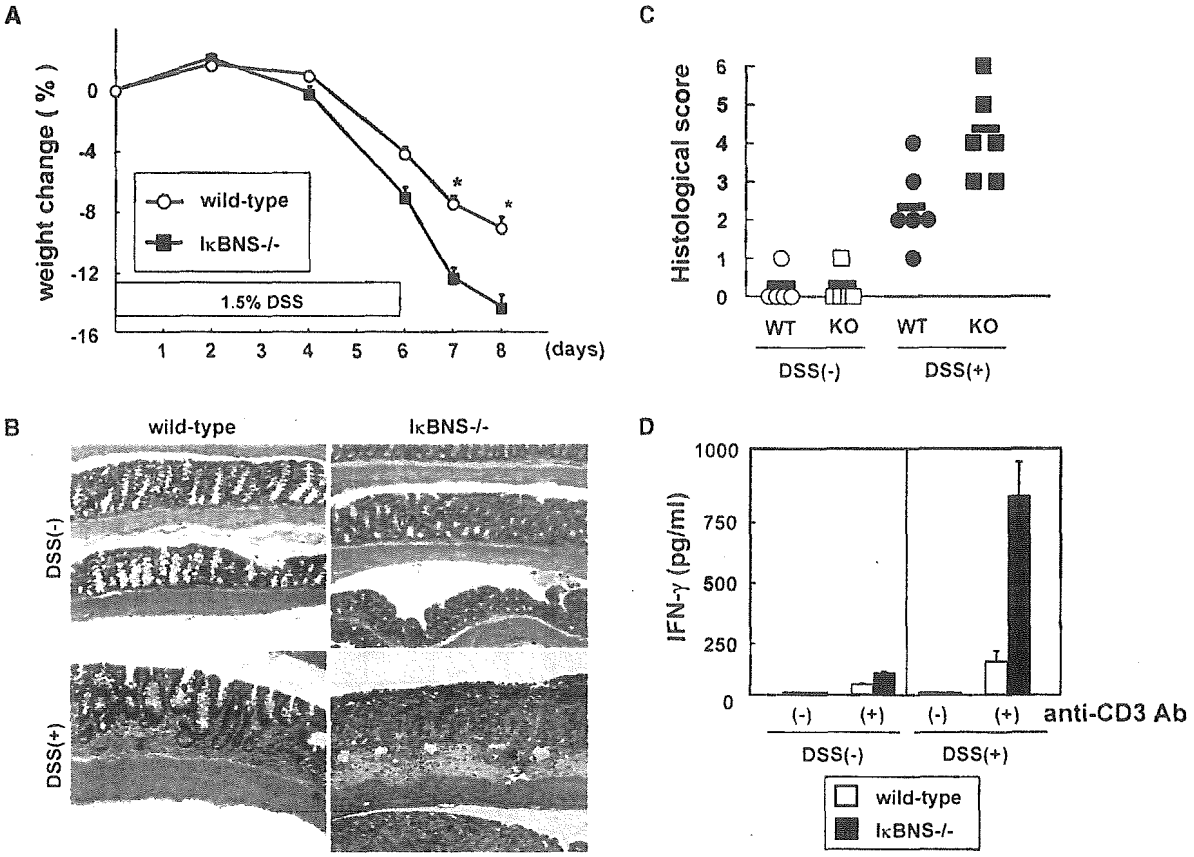

Figure 7. High Susceptibility to DSS Colitis in IκBNS$^{-/-}$ Mice

(A) Wild-type (n = 15) and IκBNS$^{-/-}$ mice (n = 15) were given 1.5% DSS in drinking water for 6 days and weighed everyday. Data are mean ± SD. *, $p < 0.05$.

(B) Histologic examination of the colons of wild-type and IκBNS$^{-/-}$ mice before or 9 days after initiation of DSS administration. H&E staining is shown. Representative of six mice examined. Magnification, 20×.

(C) The colitis scores shown for individual wild-type (circle) and IκBNS$^{-/-}$ mice (square) before (open) and after (closed) DSS treatment were total scores for individual sections as described in the Experimental Procedures section. Mean score for each group is also shown (black bar).

(D) CD4$^+$ T cells were purified from spleen of wild-type or IκBNS$^{-/-}$ mice either treated or nontreated with DSS. Then, CD4$^+$ T cells were cultured in the presence or absence of plate bound anti-CD3 Ab for 24 hr. Concentration of IFN-γ in the culture supernatants was measured by ELISA.

So far, characterized negative regulators are mainly involved in blockade of TLR signaling pathways in the cytoplasm or on the cell membrane. Accordingly, these negative regulators globally inhibit TLR-dependent gene induction. The nuclear IκB protein IκBNS is unique in that this molecule negatively regulates induction of a set of TLR-dependent genes by directly affecting NF-κB activity in the nucleus. Thus, TLR-dependent innate immune responses are regulated through a variety of mechanisms.

IκBNS-mediated inhibition of a set of TLR-dependent genes is probably explained by recruitment of IκBNS to the specific promoters. IκBNS was recruited to the IL-6 promoter, but not to the TNF-α promoter. In addition, LPS-induced recruitment of p65 to the TNF-α promoter was observed within 1 hr, whereas p65 recruitment to the IL-6 promoter was observed late, indicating that NF-κB activity was differentially regulated at both promoters. NF-κB activity at the TNF-α promoter is regulated in an IκBNS-independent manner, whereas the activity at the IL-6 promoter was IκBNS-dependent. Indeed, p65 recruitment to the TNF-α promoter was observed similarly in wild-type and IκBNS$^{-/-}$ macrophages, but the recruitment to the IL-6 promoter was sustained in IκBNS$^{-/-}$ cells. Previous reports indicate that IκBNS selectively associates with p50 subunit of NF-κB and affects NF-κB DNA binding activity (Fiorini et al., 2002; Hirotani et al., 2005). Consistent with these observations, IκBNS$^{-/-}$ macrophages showed prolonged LPS-induced NF-κB DNA binding activity and nuclear localization of p65. Taken together, these findings indicate that IκBNS, which is rapidly induced by TLR stimulation, might be recruited to gene promoters through association with p50, and contribute to termination of NF-κB activity. Termination of NF-κB activity has been shown to be induced by IKKα-mediated degradation of promoter-bound p65 (Lawrence et al., 2005). However, consistent with a recent report, we were not able to detect LPS-induced degradation of p65 in peritoneal macrophages and bone marrow-derived macrophages (Li et al., 2005). However, we could detect LPS-induced p65 degradation in the RAW264.7 macrophage cell line. In these cells, when constitutively expressed IκBNS, LPS-induced p65 turnover was

accelerated, indicating that IκBNS is involved in the degradation of promoter-bound p65. In the case of the TNF-α promoter, it is possible that NF-κB activity is already terminated when IκBNS expression is induced, and therefore IκBNS is no longer recruited to the TNF-α promoter. Alternatively, an unidentified mechanism that regulates selective recruitment of IκBNS to gene promoters might exist. The mechanisms by which IκBNS is recruited to the specific promoters through association with p50 remain unclear and would be a subject of further investigation.

Analyses of IκBNS$^{-/-}$ mice further highlighted the in vivo functions of IκBNS in limiting systemic and intestinal inflammation. IκBNS$^{-/-}$ mice succumbed to systemic LPS-induced endotoxin shock possibly due to sustained production of several TLR-dependent gene products such as IL-6 and IL-12p40. Furthermore, IκBNS$^{-/-}$ mice are more susceptible to intestinal inflammation induced by disruption of the epithelial barrier. Abnormal activation of innate immune cells caused by deficiency of IL-10 or Stat3 leads to spontaneous development of colonic inflammation (Kobayashi et al., 2003; Kuhn et al., 1993; Takeda et al., 1999). IκBNS$^{-/-}$ mice did not develop chronic colitis spontaneously until 20 week-old of age (our unpublished data). In Stat3 mutant mice, TLR-dependent production of proinflammatory cytokines increased over 10-fold compared to wild-type cells, which might contribute to the spontaneous intestinal inflammation (Takeda et al., 1999). In IκBNS$^{-/-}$ mice, increase in TLR-dependent production of proinflammatory cytokines such as IL-6 and IL-12p40 was mild compared to Stat3 mutant mice. In this case, the colonic epithelial barrier might contribute to prevention of excessive inflammatory responses in IκBNS$^{-/-}$ mice. However, when the barrier function of epithelial cells was disrupted by administration of DSS, IκBNS$^{-/-}$ mice suffered from severe intestinal inflammation accompanied by enhanced Th1 responses. IκBNS was shown to be expressed in CD11b^{+} cells residing in the colonic lamina propria (Hirotani et al., 2005). Therefore, in the absence of IκBNS, exposure of innate immune cells to intestinal microflora might result in increased or sustained production of proinflammatory cytokines such as IL-12p40, which induces exaggerated intestinal inflammation and Th1 cell development. Thus, IκBNS is responsible for the prevention of uncontrolled inflammatory responses in vivo.

In this study, we have shown that IκBNS is a selective inhibitor of TLR-dependent genes possibly through termination of NF-κB activity. Furthermore, IκBNS was responsible for prevention of inflammation through inhibition of persistent proinflammatory cytokine production. Future study that discloses the precise molecular mechanisms by which the nuclear IκB protein selectively inhibits TLR-dependent genes will provide basis for the development of new therapeutic strategies to a variety of inflammatory diseases.

Experimental Procedures

Generation of IκBNS-Deficient Mice

The *Ikbns* gene consists of eight exons (Figure 1A). The targeting vector was designed to replace a 1.8 kb fragment containing exons 5–8 of the *Ikbns* gene with a neomycin-resistance gene (*neo*). A short arm and a long arm of the homology region from the E14.1 ES genome were amplified by PCR. A herpes simplex virus thymidine kinase gene (HSV-TK) was inserted into the 3′ end of the vector. After the targeting vector was electroporated into ES cells, G418 and gancyclovir doubly resistant clones were selected and screened for homologous recombination by PCR and verified by Southern blot analysis using the probe indicated in Figure 1A. Two independently identified targeted ES clones were microinjected into C57BL/6 blastocysts. Chimeric mice were mated with C57BL/6 female mice, and heterozygous F1 progenies were intercrossed to obtain IκBNS$^{-/-}$ mice. Mice from these independent ES clones displayed identical phenotypes. All animal experiments were conducted according to guidelines of Animal Care and Use Committee at Kyushu University.

Reagents

LPS (*E. coli* 055:B5) was purchased from Sigma. Peptidoglycan was from Fluca. Pam_3CSK_4, MALP-2, and imiquimod were from Invivogen. Antibodies against p65 (C-20; sc-372), p50 (H-119; sc-7178 or NLS; sc-114), c-Rel (C; sc-71), and RNA polymerase II (H-224; sc-9001) were purchased from Santa Cruz. Rabbit anti-IκBNS Ab was generated against synthetic peptide (1-MEDSLDTRLY PEPSLSQVC-18) corresponding to N-terminal region of mouse IκBNS (MBL, Nagoya, Japan), and anti-IκBNS serum was affinity-purified using a column containing peptide-conjugated Sepharose 4B.

Preparation of Macrophages and Dendritic Cells

For isolation of peritoneal macrophages, mice were intraperitoneally injected with 2 ml of 4% thioglycollate medium (Sigma). Peritoneal exudate cells were isolated from the peritoneal cavity 3 days post injection. Cells were incubated for 2 hr and washed three times with HBSS. Remaining adherent cells were used as peritoneal macrophages for the experiments. To prepare bone marrow-derived macrophages, bone marrow cells were prepared from femora and tibia and passed through nylon mesh. Then cells were cultured in RPMI 1640 medium supplemented with 10% FCS, 100 μM 2-ME, and 10 ng/ml M-CSF (GenzymeTechne). After 6–8 days, the cells were used as macrophages for the experiments. Bone marrow-derived DCs were prepared by culturing bone marrow cells in RPMI 1640 medium supplemented with 10% FCS, 100 μM 2-ME, and 10 ng/ml GM-CSF (GenzymeTechne). After 6 days, the cells were used as DCs.

Measurement of Cytokine Production

Peritoneal macrophages or DCs were stimulated with various TLR ligands for 24 hr. Culture supernatants were collected and analyzed for TNF-α, IL-6, IL-12p40, IL-12p70, or IL-10 production with enzyme-linked immunosorbent assay (ELISA). Mice were intravenously injected with 1mg of LPS and bled at the indicated periods. Serum concentrations of TNF-α, IL-6, and IL-12p40 were determined by ELISA. ELISA kits were purchased from GenzymeTechne and R&D Systems. For measurement of IFN-γ, CD4^{+} T cells were purified from spleen cells using CD4 microbeads (Miltenyi Biotec) and stimulated by plate bound anti-CD3ε antibody (145-2C11, BD PharMingen) for 24 hr. Concentrations of IFN-γ in the supernatants were determined by ELISA (GenzymeTechne).

Quantitative Real-Time RT-PCR

Total RNA was isolated with TRIzol reagent (Invitrogen, Carlsbad, CA), and 2 μg of RNA was reverse transcribed using M-MLV reverse transcriptase (Promega, Madison, WI) and oligo (dT) primers (Toyobo, Osaka, Japan) after treatment with RQ1 DNase I (Promega). Quantitative real-time PCR was performed on an ABI 7700 (Applied Biosystems, Foster City, CA) using TaqMan Universal PCR Master Mix (Applied Biosystems). All data were normalized to the corresponding elongation factor-1α (EF-1α) expression, and the fold difference relative to the EF-1α level was shown. Amplification conditions were: 50°C (2 min), 95°C (10 min), 40 cycles of 95°C (15 s), and 60°C (60 s). Each experiment was performed independently at least three times, and the results of one representative experiment are shown. All primers were purchased from Assay on Demand (Applied Biosystems).

Electrophoretic Mobility Shift Assay

Macrophages were stimulated with 100 ng/ml LPS for the indicated periods. Then, nuclear proteins were extracted, and incubated with an end-labeled, double-stranded oligonucleotide containing an NF-κB binding site of the IL-6 promoter in 25 μl of binding buffer (10 mM HEPES-KOH, [pH 7.8], 50 mM KCl, 1 mM EDTA [pH 8.0], 5 mM $MgCl_2$ and 10% glycerol) for 20 min at room temperature and loaded on a native 5% polyacrylamide gel. The DNA-protein complexes were visualized by autoradiography.

Western Blotting

Cells were lysed with RIPA buffer (50 mM Tris-HCl [pH 7.5], 150 mM NaCl, 1% Triton X-100, 0.5% Na-deoxycholate) containing protease inhibitors (Complete Mini; Roche). The lysates were separated on SDS-PAGE and transferred to PVDF membrane. The membranes were incubated with anti-IκBα Ab, anti-ERK Ab, anti-p38 Ab, anti-JNK Ab (Santa Cruz Biotechnology), anti-phospho-p38 Ab, anti-phospho-ERK Ab, or anti-phospho-JNK Ab (Cell Signaling Technology). Bound Abs were detected with SuperSignal West Pico Chemiluminescent Substrate (Pierce).

Immunofluorescence Staining

Macrophages were stimulated with 100 ng/ml LPS for the indicated periods, washed with Tris-buffered saline (TBS), and fixed with 3.7% formaldehyde in TBS for 15 min at room temperature. After permeabilization with 0.2% Triton X-100, cells were washed with TBS and incubated with 10 ng/ml of a rabbit anti-p50 or anti-p65 Ab (Santa Cruz Biotechnology) in TBS containing 1% bovine serum albumin, followed by incubation with Alexa Fluor 594-conjugated goat anti-rabbit immunoglobulin G (IgG; Molecular Probes, Eugene, OR). To stain the nucleus, cells were cultured with 0.5 μg/ml 4, 6-diamidino-2-phenylindole (DAPI; Wako, Osaka, Japan). Stained cells were analyzed using an LSM510 model confocal microscope (Carl Zeiss, Oberkochem, Germany).

Chromatin Immunoprecipitation

Chromatin immunoprecipitation (ChIP) was performed essentially with a described protocol (Upstate Biotechnology, Lake Placid, NY). In brief, peritoneal macrophages from wild-type and $I\kappa BNS^{-/-}$ mice were stimulated with 100 ng/ml LPS for 1, 3, or 5 hr, and then fixed with formaldehyde for 10 min. The cells were lysed, sheared by sonication using Bioruptor (CosmoBio), and incubated overnight with specific antibody followed by incubation with protein A-agarose saturated with salmon sperm DNA (Upsate Biotechnology). Precipitated DNA was analyzed by quantitative PCR (35 cycles) using primers 5′- CCCCAGATTGCCACAGAATC -3′ and 5′- CCAGT GAGTGAAAGGGACAG -3′ for the TNF-α promoter and 5′- TGTGTG TCGTCTGTCATGCG-3′ and 5′- AGCTACAGACATCCCCAGTCTC -3′ for the IL-6 promoter.

Induction of DSS Colitis

Mice received 1.5% (wt/vol) DSS (40,000 kDa; ICN Biochemicals), ad libitum, in their drinking water for 6 days, then switched to regular drinking water. The amount of DSS water drank per animal was recorded and no differences in intake between strains were observed. Mice were weighed for the determination of percent weight change. This was calculated as: percentage weight change = (weight at day X-day 0/weight at day 0) × 100. Statistical significance was determined by paired Student's t test. Differences were considered to be statistically significant at $p < 0.05$.

Histological Analysis

Colon tissues were fixed in 4% paraformaldehyde, rolled up, and embedded in paraffin in a Swiss roll orientation such that the entire length of the intestinal tract could be identified on single sections. After sectioning, the tissues were dewaxed in ethanol, rehydrated, and stained hematoxylin and eosin to study histological changes after DSS-induced damage. Histological scoring was performed in a blinded fashion by a pathologist, with a combined score for inflammatory cell infiltration (score, 0–3) and tissue damage (score, 0–3) (Araki et al., 2005). The presence of occasional inflammatory cells in the lamina propria was assigned a value of 0; increased numbers of inflammatory cells in the lamina propria as 1; confluence of inflammatory cells, extending into the submucosa, as 2; and transmural extension of the infiltrate as 3. For tissue damage, no mucosal damage was scored as 0; discrete lymphoepithelial lesions were scored as 1; surface mucosal erosion or focal ulceration was scored as 2; and extensive mucosal damage and extension into deeper structures of the bowel wall were scored as 3. The combined histological score ranged from 0 (no changes) to 6 (extensive cell infiltration and tissue damage).

Supplemental Data

Supplemental Data include four figures and are available with this article online at http://www.immunity.com/cgi/content/full/24/1/41/DC1/.

Acknowledgments

We thank Y. Yamada, K. Takeda, M. Otsu, and N. Kinoshita for technical assistance; M. Yamamoto and S. Akira for providing us with reagents, P. Lee for critical reading of the manuscript, and M. Kurata for secretarial assistance. This work was supported by grants from the Special Coordination Funds of the Ministry of Education, Culture, Sports, Science and Technology; the Uehara Memorial Foundation; the Mitsubishi Foundation; the Takeda Science Foundation; the Tokyo Biochemical Research Foundation; the Kowa Life Science Foundation; the Osaka Foundation for Promotion of Clinical Immunology; and the Sankyo Foundation of Life Science.

Received: July 15, 2005
Revised: September 16, 2005
Accepted: November 16, 2005
Published: January 17, 2006

References

Akira, S., and Takeda, K. (2004). Toll-like receptor signalling. Nat. Rev. Immunol. *4*, 499–511.

Araki, A., Kanai, T., Ishikura, T., Makita, S., Uraushihara, K., Iiyama, R., Totsuka, T., Takeda, K., Akira, S., and Watanabe, M. (2005). MyD88-deficient mice develop severe intestinal inflammation in dextran sodium sulfate colitis. J. Gastroenterol. *40*, 16–23.

Beutler, B. (2004). Inferences, questions and possibilities in Toll-like receptor signalling. Nature *430*, 257–263.

Bjorkbacka, H., Kunjathoor, V.V., Moore, K.J., Koehn, S., Ordija, C.M., Lee, M.A., Means, T., Halmen, K., Luster, A.D., Golenbock, D.T., and Freeman, M.W. (2004). Reduced atherosclerosis in MyD88-null mice links elevated serum cholesterol levels to activation of innate immunity signaling pathways. Nat. Med. *10*, 416–421.

Boone, D.L., Turer, E.E., Lee, E.G., Ahmad, R.C., Wheeler, M.T., Tsui, C., Hurley, P., Chien, M., Chai, S., Hitotsumatsu, O., et al. (2004). The ubiquitin-modifying enzyme A20 is required for termination of Toll-like receptor responses. Nat. Immunol. *5*, 1052–1060.

Brint, E.K., Xu, D., Liu, H., Dunne, A., McKenzie, A.N., O'Neill, L.A., and Liew, F.Y. (2004). ST2 is an inhibitor of interleukin 1 receptor and Toll-like receptor 4 signaling and maintains endotoxin tolerance. Nat. Immunol. *5*, 373–379.

Burns, K., Janssens, S., Brissoni, B., Olivos, N., Beyaert, R., and Tschopp, J. (2003). Inhibition of interleukin 1 receptor/Toll-like receptor signaling through the alternatively spliced, short form of MyD88 is due to its failure to recruit IRAK-4. J. Exp. Med. *197*, 263–268.

Chuang, T.H., and Ulevitch, R.J. (2004). Triad3A, an E3 ubiquitin-protein ligase regulating Toll-like receptors. Nat. Immunol. *5*, 495–502.

Diehl, G.E., Yue, H.H., Hsieh, K., Kuang, A.A., Ho, M., Morici, L.A., Lenz, L.L., Cado, D., Riley, L.W., and Winoto, A. (2004). TRAIL-R as a negative regulator of innate immune cell responses. Immunity *21*, 877–889.

Divanovic, S., Trompette, A., Atabani, S.F., Madan, R., Golenbock, D.T., Visintin, A., Finberg, R.W., Tarakhovsky, A., Vogel, S.N., Belkaid, Y., et al. (2005). Negative regulation of Toll-like receptor 4 signaling by the Toll-like receptor homolog RP105. Nat. Immunol. *6*, 571–578.

Eriksson, U., Ricci, R., Hunziker, L., Kurrer, M.O., Oudit, G.Y., Watts, T.H., Sonderegger, I., Bachmaier, K., Kopf, M., and Penninger, J.M.

(2003). Dendritic cell-induced autoimmune heart failure requires cooperation between adaptive and innate immunity. Nat. Med. *9*, 1484–1490.

Fiorini, E., Schmitz, I., Marissen, W.E., Osborn, S.L., Touma, M., Sasada, T., Reche, P.A., Tibaldi, E.V., Hussey, R.E., Kruisbeek, A.M., et al. (2002). Peptide-induced negative selection of thymocytes activates transcription of an NF-kappa B inhibitor. Mol. Cell *9*, 637–648.

Fukao, T., Tanabe, M., Terauchi, Y., Ota, T., Matsuda, S., Asano, T., Kadowaki, T., Takeuchi, T., and Koyasu, S. (2002). PI3K-mediated negative feedback regulation of IL-12 production in DCs. Nat. Immunol. *3*, 875–881.

Hirotani, T., Lee, P.Y., Kuwata, H., Yamamoto, M., Matsumoto, M., Kawase, I., Akira, S., and Takeda, K. (2005). The nuclear IkappaB protein IkappaBNS selectively inhibits lipopolysaccharide-induced IL-6 production in macrophages of the colonic lamina propria. J. Immunol. *174*, 3650–3657.

Honda, K., Yanai, H., Negishi, H., Asagiri, M., Sato, M., Mizutani, T., Shimada, N., Ohba, Y., Takaoka, A., Yoshida, N., and Taniguchi, T. (2005). IRF-7 is the master regulator of type-I interferon-dependent immune responses. Nature *434*, 772–777.

Iwasaki, A., and Medzhitov, R. (2004). Toll-like receptor control of the adaptive immune responses. Nat. Immunol. *5*, 987–995.

Kawai, T., Adachi, O., Ogawa, T., Takeda, K., and Akira, S. (1999). Unresponsiveness of MyD88-deficient mice to endotoxin. Immunity *11*, 115–122.

Kinjyo, I., Hanada, T., Inagaki-Ohara, K., Mori, H., Aki, D., Ohishi, M., Yoshida, H., Kubo, M., and Yoshimura, A. (2002). SOCS1/JAB is a negative regulator of LPS-induced macrophage activation. Immunity *17*, 583–591.

Kisielow, P., Bluthmann, H., Staerz, U.D., Steinmetz, M., and von Boehmer, H. (1988). Tolerance in T-cell-receptor transgenic mice involves deletion of nonmature CD4+8+ thymocytes. Nature *333*, 742–746.

Kitajima, S., Takuma, S., and Morimoto, M. (1999). Changes in colonic mucosal permeability in mouse colitis induced with dextran sulfate sodium. Exp. Anim. *48*, 137–143.

Kobayashi, K., Hernandez, L.D., Galan, J.E., Janeway, C.A., Jr., Medzhitov, R., and Flavell, R.A. (2002). IRAK-M is a negative regulator of Toll-like receptor signaling. Cell *110*, 191–202.

Kobayashi, M., Kweon, M.N., Kuwata, H., Schreiber, R.D., Kiyono, H., Takeda, K., and Akira, S. (2003). Toll-like receptor-dependent production of IL-12p40 causes chronic enterocolitis in myeloid cell-specific Stat3-deficient mice. J. Clin. Invest. *111*, 1297–1308.

Kuhn, R., Lohler, J., Rennick, D., Rajewsky, K., and Muller, W. (1993). Interleukin-10-deficient mice develop chronic enterocolitis. Cell *75*, 263–274.

Kuwata, H., Watanabe, Y., Miyoshi, H., Yamamoto, M., Kaisho, T., Takeda, K., and Akira, S. (2003). IL-10-inducible Bcl-3 negatively regulates LPS-induced TNF-alpha production in macrophages. Blood *102*, 4123–4129.

Lang, K.S., Recher, M., Junt, T., Navarini, A.A., Harris, N.L., Freigang, S., Odermatt, B., Conrad, C., Ittner, L.M., Bauer, S., et al. (2005). Toll-like receptor engagement converts T-cell autoreactivity into overt autoimmune disease. Nat. Med. *11*, 138–145.

Lawrence, T., Bebien, M., Liu, G.Y., Nizet, V., and Karin, M. (2005). IKKalpha limits macrophage NF-kappaB activation and contributes to the resolution of inflammation. Nature *434*, 1138–1143.

Leadbetter, E.A., Rifkin, I.R., Hohlbaum, A.M., Beaudette, B.C., Shlomchik, M.J., and Marshak-Rothstein, A. (2002). Chromatin-IgG complexes activate B cells by dual engagement of IgM and Toll-like receptors. Nature *416*, 603–607.

Li, Q., Lu, Q., Bottero, V., Estepa, G., Morrison, L., Mercurio, F., and Verma, I.M. (2005). Enhanced NF-(kappa)B activation and cellular function in macrophages lacking I(kappa)B kinase 1 (IKK1). Proc. Natl. Acad. Sci. USA *102*, 12425–12430.

Liew, F.Y., Xu, D., Brint, E.K., and O'Neill, L.A. (2005). Negative regulation of Toll-like receptor-mediated immune responses. Nat. Rev. Immunol. *5*, 446–458.

Michelsen, K.S., Wong, M.H., Shah, P.K., Zhang, W., Yano, J., Doherty, T.M., Akira, S., Rajavashisth, T.B., and Arditi, M. (2004). Lack of Toll-like receptor 4 or myeloid differentiation factor 88 reduces atherosclerosis and alters plaque phenotype in mice deficient in apolipoprotein E. Proc. Natl. Acad. Sci. USA *101*, 10679–10684.

Moore, K.W., de Waal Malefyt, R., Coffman, R.L., and O'Garra, A. (2001). Interleukin-10 and the interleukin-10 receptor. Annu. Rev. Immunol. *19*, 683–765.

Motoyama, M., Yamazaki, S., Eto-Kimura, A., Takeshige, K., and Muta, T. (2005). Positive and negative regulation of nuclear factor-kappaB-mediated transcription by IkappaB-zeta, an inducible nuclear protein. J. Biol. Chem. *280*, 7444–7451.

Nakagawa, R., Naka, T., Tsutsui, H., Fujimoto, M., Kimura, A., Abe, T., Seki, E., Sato, S., Takeuchi, O., Takeda, K., et al. (2002). SOCS-1 participates in negative regulation of LPS responses. Immunity *17*, 677–687.

Natoli, G., Saccani, S., Bosisio, D., and Marazzi, I. (2005). Interactions of NF-kappaB with chromatin: the art of being at the right place at the right time. Nat. Immunol. *6*, 439–445.

Pasare, C., and Medzhitov, R. (2004). Toll-dependent control mechanisms of CD4 T cell activation. Immunity *21*, 733–741.

Saccani, S., Marazzi, I., Beg, A.A., and Natoli, G. (2004). Degradation of promoter-bound p65/RelA is essential for the prompt termination of the nuclear factor kappaB response. J. Exp. Med. *200*, 107–113.

Sakaguchi, S., Negishi, H., Asagiri, M., Nakajima, C., Mizutani, T., Takaoka, A., Honda, K., and Taniguchi, T. (2003). Essential role of IRF-3 in lipopolysaccharide-induced interferon-beta gene expression and endotoxin shock. Biochem. Biophys. Res. Commun. *306*, 860–866.

Strober, W., Fuss, I.J., and Blumberg, R.S. (2002). The immunology of mucosal models of inflammation. Annu. Rev. Immunol. *20*, 495–549.

Takaoka, A., Yanai, H., Kondo, S., Duncan, G., Negishi, H., Mizutani, T., Kano, S., Honda, K., Ohba, Y., Mak, T.W., and Taniguchi, T. (2005). Integral role of IRF-5 in the gene induction programme activated by Toll-like receptors. Nature *434*, 243–249.

Takeda, K., Clausen, B.E., Kaisho, T., Tsujimura, T., Terada, N., Forster, I., and Akira, S. (1999). Enhanced Th1 activity and development of chronic enterocolitis in mice devoid of Stat3 in macrophages and neutrophils. Immunity *10*, 39–49.

Wald, D., Qin, J., Zhao, Z., Qian, Y., Naramura, M., Tian, L., Towne, J., Sims, J.E., Stark, G.R., and Li, X. (2003). SIGIRR, a negative regulator of Toll-like receptor-interleukin 1 receptor signaling. Nat. Immunol. *4*, 920–927.

Wesselis, J., Baer, M., Young, H.A., Claudio, E., Brown, K., Siebenlist, U., and Johnson, P.F. (2004). BCL-3 and NF-kappaB p50 attenuate lipopolysaccharide-induced inflammatory responses in macrophages. J. Biol. Chem. *279*, 49995–50003.

Yamamoto, M., Sato, S., Hemmi, H., Hoshino, K., Kaisho, T., Sanjo, H., Takeuchi, O., Sugiyama, M., Okabe, M., Takeda, K., and Akira, S. (2003). Role of adaptor TRIF in the MyD88-independent toll-like receptor signaling pathway. Science *301*, 640–643.

Yamamoto, M., Yamazaki, S., Uematsu, S., Sato, S., Hemmi, H., Hoshino, K., Kaisho, T., Kuwata, H., Takeuchi, O., Takeshige, K., et al. (2004). Regulation of Toll/IL-1-receptor-mediated gene expression by the inducible nuclear protein IkappaBzeta. Nature *430*, 218–222.

The Nuclear IκB Protein IκBNS Selectively Inhibits Lipopolysaccharide-Induced IL-6 Production in Macrophages of the Colonic Lamina Propria[1]

Tomonori Hirotani,*† Pui Y. Lee,*¶ Hirotaka Kuwata,§ Masahiro Yamamoto,*‡ Makoto Matsumoto,§ Ichiro Kawase,† Shizuo Akira,*‡ and Kiyoshi Takeda[2§]

Macrophages play an important role in the pathogenesis of chronic colitis. However, it remains unknown how macrophages residing in the colonic lamina propria are regulated. We characterized colonic lamina proprial CD11b-positive cells (CLPMϕ). CLPMϕ of wild-type mice, but not IL-10-deficient mice, displayed hyporesponsiveness to TLR stimulation in terms of cytokine production and costimulatory molecule expression. We compared CLPMϕ gene expression profiles of wild-type mice with IL-10-deficient mice, and identified genes that are selectively expressed in wild-type CLPMϕ. These genes included nuclear IκB proteins such as Bcl-3 and IκBNS. Because Bcl-3 has been shown to specifically inhibit LPS-induced TNF-α production, we analyzed the role of IκBNS in macrophages. Lentiviral introduction of IκBNS resulted in impaired LPS-induced IL-6 production, but not TNF-α production in the murine macrophage cell line RAW264.7. IκBNS expression led to constitutive and intense DNA binding of NF-κB p50/p50 homodimers. IκBNS was recruited to the IL-6 promoter, but not to the TNF-α promoter, together with p50. Furthermore, small interference RNA-mediated reduction in IκBNS expression in RAW264.7 cells resulted in increased LPS-induced production of IL-6, but not TNF-α. Thus, IκBNS selectively suppresses LPS-induced IL-6 production in macrophages. This study established that nuclear IκB proteins differentially regulate LPS-induced inflammatory cytokine production in macrophages. ***The Journal of Immunology,*** **2005, 174: 3650–3657.**

Inflammatory bowel diseases (IBD)[3] including Crohn's disease and ulcerative colitis are chronic immune-mediated disorders for which pathogenesis and etiology are poorly understood (1). A number of animal models of mucosal inflammation have been developed to analyze the pathogenesis of IBD (2, 3). In the course of analyzing these models, many types of cells including T cells, B cells, and epithelial cells have been shown to contribute to the pathogenesis of colitis. Among these cell populations, T cells have been shown to possess effector and regulatory functions in the development of chronic colitis. Both $CD4^+$ Th1 and Th2 cells are critically involved in mucosal immunity as effector cells, and disrupting the balance of Th1/Th2 polarization leads to the development of chronic mucosal inflammation (4). Crohn's disease is considered to be a Th1-dependent inflammatory disease, whereas ulcerative colitis is a Th2-dependent disease (3). In addition, regulatory T cells, such as $CD25^+CD4^+$ T cells, TGF-β-producing Th3 cells, and IL-10-producing type 1 regulatory T cells, all have regulatory functions in prevention of chronic mucosal inflammation and even in amelioration of established colitis (5, 6). B cells also have regulatory functions in mucosal inflammation observed in TCR-α-deficient mice (7). Thus, important roles of adaptive immunity comprising T cells and B cells in mucosal inflammation are well characterized.

However, recent accumulating evidence demonstrates that innate immunity plays crucial roles in controlling Ag-specific adaptive immunity (8–11). Accordingly, the involvement of innate immunity in the development of chronic colitis has been proposed. Abnormal activation of innate immune cells has been shown to initiate the development of chronic colitis in mice lacking Stat3 specifically in macrophages and neutrophils (12). The phenotype observed in the Stat3 mutant mice was very reminiscent of that observed in IL-10-deficient mice, indicating that major target cells of IL-10 in suppressing chronic mucosal inflammation are cells of macrophage lineage (12–14). The mechanisms by which abnormal activity of innate immune cells leads to the development of chronic colitis were further analyzed. In the absence of Stat3, innate immune cells showed increased levels of inflammatory cytokine production through TLR, which are essential for the recognition of microbial components in innate immune cells. Among these cytokines, IL-12p40 is responsible for the exaggerated Th1 cell development and thereby induces Th1-dependent chronic colitis (15). Thus, critical involvement of TLR-dependent activation of innate immunity has clearly been shown in triggering chronic mucosal inflammation. In addition to TLR-mediated activation of innate immunity, NOD2, which is responsible for TLR-independent recognition of microbial components, has been implicated in the pathogenesis of Crohn's disease in human (16–18). Thus, molecules critically involved in innate immune responses, such as TLRs

*Department of Host Defense, Research Institute for Microbial Diseases and †Department of Molecular Medicine, Graduate School of Medicine, Osaka University, and ‡Exploratory Research for Advanced Technology, Japan Science and Technology Agency, Osaka, Japan; §Department of Molecular Genetics, Medical Institute of Bioregulation, Kyushu University, Fukuoka, Japan; and ¶Department of Medicine, Division of Rheumatology and Clinical Immunology, University of Florida, Gainesville, FL 32610

Received for publication October 5, 2004. Accepted for publication January 11, 2005.

The costs of publication of this article were defrayed in part by the payment of page charges. This article must therefore be hereby marked *advertisement* in accordance with 18 U.S.C. Section 1734 solely to indicate this fact.

[1] This work was supported by grants from the Special Coordination Funds of the Ministry of Education, Culture, Sports, Science and Technology.

[2] Address correspondence and reprint requests to Dr. Kiyoshi Takeda, Department of Molecular Genetics, Medical Institute of Bioregulation, Kyushu University, 3-1-1 Maidashi, Higashi-ku, Fukuoka 812-8582, Japan. E-mail address: ktakeda@bioreg.kyushu-u.ac.jp

[3] Abbreviations used in this paper: IBD, inflammatory bowel disease; CLPMϕ, colonic lamina proprial CD11b-positive cell; ChIP, chromatin immunoprecipitation; siRNA, small interference RNA.

0022-1767/05/$02.00

and NOD2, are associated with the pathogenesis of colitis. However, it remains unclear how activities of these innate immune cell populations are regulated in the intestinal mucosa.

In this study, we isolated CD11b-positive cells from the colonic lamina propria (CLPMϕ), and analyzed their responsiveness to TLR ligands. CLPMϕ of wild-type mice, but not IL-10-deficient mice, showed hyporesponsiveness to TLR ligands. Therefore, we compared CLPMϕ gene expression profiles in wild-type mice with IL-10-deficient mice, which led to identification of genes that are specifically expressed in CLPMϕ of wild-type mice, but not in CLPMϕ of IL-10-deficient mice or wild-type peritoneal macrophages. We further analyzed whether these gene products are capable of inhibiting TLR-mediated responses in macrophages, and found that a member of the IκB family of proteins, IκBNS, inhibits LPS-induced IL-6 production in macrophages.

Materials and Methods

Reagents and cell culture

LPS from *Escherichia coli* (O55:B5) was purchased from Sigma-Aldrich. The mouse macrophage cell line (RAW264.7) and human embryonic kidney 293T cells were cultured in DMEM supplemented with 10% FBS, 100 μg/ml streptomycin, and 10 U/ml penicillin G. Mouse peritoneal macrophages were collected by peritoneal lavage with HBSS at 3 days after i.p. injection of 2 ml of 4% sterile thioglycolate into 8- to 12-wk-old mice. Peritoneal macrophages were cultured in RPMI 1640 medium with 10% FBS, 100 μg/ml streptomycin, and 10 U/ml penicillin G.

Mice

C57BL/6 mice were purchased from the Central Laboratory of Experimental Animals (Tokyo, Japan). IL-10-deficient mice were purchased from The Jackson Laboratory. All experiments using these mice were approved by and performed according to the guidelines of the animal ethics committee of Kyushu University and Osaka University.

Isolation of CLPMϕ

CLPMϕ was isolated using a protocol modified from an EDTA perfusion method (19). Mice were anesthetized and their peritoneal and pleural cavities were opened for systemic perfusion from left ventricle with 15 ml of HBSS containing 20 mM EDTA. Following perfusion, colons were removed, cut into pieces of 2~3 cm in length, resuspended in HBSS, and shaken with a microbead beater (Biospec Products) at 5000 rpm for 50 s to remove epithelial cells. The colon pieces were then washed with RPMI 1640, mechanically minced and resuspended in RPMI 1640 supplemented with 10% FBS, 2 mg/ml collagenase type II (Invitrogen Life Technologies), 1 mg/ml dispase (Invitrogen Life Technologies), 15 mg/ml DNase (Boehringer), 100 μg/ml streptomycin, and 10 U/ml penicillin G for 30 min at 37°C in a shaking incubator. After filtration of digested tissue with 40-μm nylon mesh, isolated cells were washed with PBS and CD11b-positive cells were purified using MACS selection system using CD11b MicroBeads (Miltenyi Biotec) following manufacturer's instructions.

Measurement of inflammatory cytokines

The cells (5×10^4) were cultured in 96-well plates with 10 or 100 ng/ml LPS for 24 h. The concentrations of TNF-α, IL-6, and IL-12p40 in the culture supernatants were determined by ELISA according to the manufacturer's instructions (Genzyme Techne).

Flow cytometry

Single cell suspension of colonic lamina propria was stained with PE-conjugated anti-CD11b Ab (BD Pharmingen) and biotin-conjugated anti-TLR4/MD-2 Ab (eBioscience), followed by FITC-conjugated streptavidin. Stained cells were analyzed on a FACSCalibur (BD Biosciences).

DNA microarray

Total RNA from wild-type or IL-10-deficient lamina proprial CD11b-positive cells was extracted with an RNeasy kit (Qiagen), followed by mRNA purification with an Oligotex mRNA kit (Amersham Pharmacia Biotech). Double-stranded cDNA was synthesized from 1 μg of mRNA with the SuperScript Choice System (Invitrogen Life Technologies) primed with T7-oligo(dT) 24 primer. These cDNA were used to prepare biotin-labeled cRNA by an in vitro transcription reaction using T7 RNA polymerase in the presence of biotinylated ribonucleotides, according to the manufacturer's protocol (Enzo Diagnostics). The cRNA products were purified using an RNeasy kit (Qiagen), fragmented, and hybridized to Affymetrix Murine Genome U74Av2, Bv2 and Cv2 microarray chips, according to the manufacturer's protocol (Affymetrix). The hybridized chips were stained, washed, and scanned with a GeneArray scanner (Affymetrix).

RT-PCR

Total RNA (1 μg) was primed with random hexamers, followed by reverse transcription with Superscript II (Invitrogen Life Technologies). PCR analysis was performed using recombinant TaqDNA polymerase (Takara Shuzo). Conditions for the reactions were 30 s of denaturation step at 94°C, 30 s of annealing step at 60°C, and 1 min of elongation step at 72°C for 25–30 cycles. Specific primers used were: IκBNS, sense 5′-GCTGTATC CTGAGCCTTCCCTGTC-3′ and antisense 5′-GCTCAGCAGGTCTTC CACAATCAG-3′; IκBζ, sense 5′-GCTCAACCTGGCTTACTTCTAC GG-3′ and antisense 5′-CGGAAGCCTTCTGCTTGTTGCTTC-3′; Bcl-3, sense 5′-GATGCCCATTTACTCTACCCCGAC-3′ and antisense 5′-GC CGGACCATGTCTGGTAATGTGG-3′; CD163, sense 5′-CTTCTTGGAG GTGCTGGATCTCCTG-3′ and antisense 5′-GCTCCCTCTAAGCAAAT CACACCG-3′; macrophage scavenger receptor 2, sense 5′GGTGCTGG AAACAGCTCTTGGAC-3′ and antisense 5′-GCTCAGCAGGTCTTCCA CAATCAG-3′; β-actin, sense 5′-CTATGTGGGTGACGAGGCCCAGAG-3′ and antisense 5′-GGGTACATGGTGGTACCACCAGAC-3′.

Real-time PCR

RAW264.7 cells and murine peritoneal macrophages were treated with 10 ng/ml IL-10 (Genzyme) for 1, 2, 4, or 6 h. Total RNA was isolated with TRIzol (Invitrogen Life Technologies) and treated with DNaseI (Promega). Reverse transcription was performed using MMLV Reverse Transcriptase (Promega) and oligo(dT) primers (Promega). Finally these solutions were directly used as templates for PCR. Quantitative real-time PCR was performed on an ABI 7000 sequence detection system (Applied Biosystems) using TaqMan universal PCR Master Mix (Applied Biosystems), as previously described (20). TaqMan probes mix for IκBNS was purchased from Applied Biosystems. All data were normalized to EF1-α expression in the same cDNA set.

Lentiviral introduction of IκBNS into macrophages

The lentiviral vector, CSII-EF-MCS-IRES-hrGFP (cPPT-containing SIN vector plasmid with multiple cloning sites for cDNA insertion followed by the IRES-GFP sequence under the control of the EF-1α promoter), was used to generate CSII-EF-IκBNS. Woodchuck hepatitis virus posttranslational regulatory element was ligated at the 3′ end of GFP. The lentiviral vectors were cotransfected into 293T cells with pMDLg/pRRE (packaging plasmid), pRSV-Rev (Rev expression plasmid), and pMD.G (VSV-G expression plasmid). Infectious lentiviruses in the culture supernatants were harvested at 48 h after transfection. RAW cells (5×10^5) were cultured with the lentiviruses for 24 h, and then the culture medium was replaced. After 48 h, the cells expressing human recombinant GFP were sorted by FACSVantage SE (BD Biosciences).

Northern blot analysis

The cells were stimulated with 100 ng/ml LPS. Total RNA was extracted using TRIzol reagent (Invitrogen Life Technologies), electrophoresed, transferred to a nylon membrane, and hybridized with cDNA probe.

Western blot analysis

Cells (2×10^6) were lysed with lysis buffer containing with 20 mM Tris-HCl, pH 7.5, 150 mM NaCl, 1% Nonidet P-40, and Complete Mini (Roche). The lysates were separated on SDS-PAGE and transferred to polyvinylidene fluoride membrane. The membranes were incubated with anti-Flag M2 Ab (Sigma-Aldrich), anti-IκBα Ab, anti-ERK Ab, anti-p38 Ab (Santa Cruz Biotechnology), anti-phospho-p38 Ab, and anti-phospho-ERK Ab (Cell Signaling Technology). Bound Abs were detected with an ECL system (PerkinElmer).

Immunoprecipitation

The cell lysates were precleared with protein G-Sepharose beads (Amersham Pharmacia Biotech) and then incubated with protein G-Sepharose beads together with anti-Flag M2 Ab, anti-p50 Ab, and anti-p65 Ab (Santa Cruz Biotechnology). Immunoprecipitates were separated on SDS-PAGE, transferred to polyvinylidene fluoride membrane, and incubated anti-Flag M2 Ab, anti-p50 Ab, or anti-p65 Ab. Bound Abs were visualized with an ECL system (PerkinElmer).